CAPITAL UNIVERSITY OF SCIENCE AND
TECHNOLOGY, ISLAMABAD

Impact Resistance of Concrete Wall having Jute Fibers and GFRP Rebars

by

Shehryar Ahmed

A thesis submitted in partial fulfillment for the
degree of Master of Science

in the

Faculty of Engineering
Department of Civil Engineering

May 2020

This effort is dedicated to my respected and affectionate parents, who helped me through all difficult times of my life, always prayed for my achievements, sacrificed all the comforts of their lives for my bright future and blessed me with their ethical support at all times. This is also a tribute to my honorable teachers who guided me to face the challenges of life with patience and courage, and who made me what I am today.

CERTIFICATE OF APPROVAL

Impact Resistance of Concrete Wall having Jute Fibers and GFRP Rebars

by

Shehryar Ahmed

(MCE183019)

THESIS EXAMINING COMMITTEE

S. No.	Examiner	Name	Organization
(a)	External Examiner	Engr. Dr. Rao Arsalan Khushnood	NUST, Islamabad
(b)	Internal Examiner	Engr. Dr. Ishtiaq Hassan	CUST, Islamabad
(c)	Supervisor	Engr. Prof. Dr. Majid Ali	CUST, Islamabad

Engr. Prof. Dr. Majid Ali
Thesis Supervisor
May 2020

Engr. Dr. Ishtiaq Hassan
Head
Dept. of Civil Engineering
May 2020

Engr. Dr. Imtiaz Ahmed Taj
Dean
Faculty of Engineering
May 2020

Author's Declaration

I, **Shehryar Ahmed** hereby state that my MS thesis titled "**Impact Resistance of Concrete Wall having Jute Fibers and GFRP Rebars**" is my own work and has not been submitted previously by me for taking any degree from Capital University of Science and Technology, Islamabad or anywhere else in the country/abroad.

At any time if my statement is found to be incorrect even after my graduation, the University has the right to withdraw my MS Degree.

(Shehryar Ahmed)

Registration No: MCE183019

Plagiarism Undertaking

I solemnly declare that research work presented in this thesis titled "**Impact Resistance of Concrete Wall having Jute Fibers and GFRP Rebars**" is solely my research work with no significant contribution from any other person. Small contribution/help wherever taken has been acknowledged and that complete thesis has been written by me.

I understand the zero tolerance policy of the HEC and Capital University of Science and Technology towards plagiarism. Therefore, I as an author of the above titled thesis declare that no portion of my thesis has been plagiarized and any material used as reference is properly referred/cited.

I undertake that if I am found guilty of any formal plagiarism in the above titled thesis even after award of MS Degree, the University reserves the right to withdraw/revoke my MS degree and that HEC and the University have the right to publish my name on the HEC/University website on which names of students are placed who submitted plagiarized work.

(Shehryar Ahmed)

Registration No: MCE183019

List of Publications

It is certified that following publication(s) have been made out of the research work that has been carried out for this thesis:-

ISI Impact Factor Article

1. Ahmed, S. and Ali, M. (2020).Use of agriculture waste as short discrete fibers and glass-fiber-reinforced-polymer rebars in concrete walls for enhancing impact resistance. *Journal of Cleaner Production*, 20th May, 122211. (ISI Impact Factor = 6.395, W-Platinum category).
   https://doi.org/10.1016/j.jclepro.2020.122211

International Refereed Conference Articles

1. Ahmed, S. and Ali, M. (2019). Impact resistance investigation of fibre reinforced concrete having GFRP rebars in last two decades. *Proceedings of 2nd International Conference on Sustainable Development in Civil Engineering*, MUET, Jamshoro, Sindh, Pakistan. December 05-07, Paper 214.

2. Ahmed, S. and Ali, M. (2020).Improvement in impact resistance of GFRP rebars reinforced concrete wall panels using jute fibres. *Proceedings of 11th International Civil Engineering Conference*, NED, Karachi, Pakistan. March 13-14, Paper 18.

(Shehryar Ahmed)

Registration No: MCE183019

Acknowledgements

First and above all, I am humbly grateful to Almighty ALLAH, for giving me the opportunity and blessing me the capability to progress successfully.

I would like to express my sincere thanks and gratefulness to **Engr. Prof. Dr. Majid Ali**. His valuable guidance, advice and encouragement helped me a lot in completing this research work. It is really an honor for me to work on the concept of impact resistance using fibre reinforced concrete. His contribution in training me as a researcher is highly appreciated.

I am grateful to all members of structural material research group (SMaRG) for their valuable assistance throughout that led to the successful completion of this research work. I am highly indebted to my father Engr. Muhammad Banaras Paracha who assisted me in developing the impact testing apparatus that has aided in making my research output worthy.

Lastly and foremost, I extend my thanks to my family and friends, for their prayers, guidance and encouragement throughout this degree.

(Shehryar Ahmed)

Registration No: MCE183019

Abstract

Residual wastes of large-scale productions are constantly gaining the attention in developing countries for their possible use in the manufacturing of sustainable materials. Use of fibers (especially natural fibers that are abundantly available in agriculturally progressive countries) in concrete can engage the construction industry for adopting environmentally friendly material composites. Jute fibers have the tendency to improve the performance of concrete in terms of energy absorption. Structures that are vulnerable to blast happenings are supposed to absorb the high impact energy in case of such unprecedented event.

In current study, the impact resistance of concrete walls having jute fibers as additives and GFRP rebars as replacement of steel rebars is investigated. A total of 16 walls of size 375 mm x 375 mm x 50 mm are prepared having combinations of steel rebars and GFRP rebars with normal concrete and jute fiber reinforced concrete. 50 mm jute fibers are used, 5% by mass of cement. Rebars of diameter 6 mm are used. Mix design ratio of 1: 2: 3: 0.6 (Cement: Sand: Aggregates: w/c) is taken. Impact tests are conducted using modified pendulum impact apparatus in two categories, i.e. low impact and high impact, . The outcomes of S-RC are assigned a reference value 100% with respect to which results of other combinations are reported in terms of percentage increment and decrement. Basic dynamic properties are calculated before impact strength, after initial cracking and after ultimate failure. SEM imaging is utilized for the analysis of post impact fiber concrete bond condition.

The obtained impact results and damping percentages show the domination of GFRP rebars reinforced concrete walls having jute fibers over other combinations in terms of toughness and impact resistance. Developed empirical equation can be utilized to observe trend of damping using the impact strength. GFRP rebars reinforced concrete wall having jute fibers has greater moment and impact load capacity as compared to other combinations. Strong fiber concrete bond poses greater resistance to defragmentation of concrete. A detailed research program

is needed to investigate other aspects of jute fiber reinforced concrete such as durability for commercial implementation in construction industry.

Contents

List of Figures

List of Tables

Abbreviations

$\mathbf{A}_f$	Cross-sectional Area of Rebar
b	Unit Width
$\mathbf{c}$ / $\mathbf{c}_b$	Depth of Compression Zone at Balanced Strain Condition
CFRC	Coconut Fiber Reinforced Concrete
d	Effective Depth
$\mathbf{E}_\alpha$	Energy Absorption till Maximum Load
$\mathbf{E}_\beta$	Cracked Energy Absorption till Ultimate Failure
$\mathbf{E}_T$	Total Energy Absorption
$\mathbf{EM}_d$	Dynamic Elastic Modulus
$\mathbf{f}_c$'	Concrete Crushing Strength under Compression
$\mathbf{f}_n$	Fundamental Period
$\mathbf{f}_y$	Strength of Steel Rebar at Yielding
FRC	Fiber Reinforced Concrete
FRP	Fiber Reinforced Polymer
FS	First Strike
GFRP-RC	Glass Fiber Reinforced Polymer Rebars Reinforced Concrete
GFRP-RC + JF	Glass Fiber Reinforced Polymer Rebars Reinforced Concrete having Jute Fibers
IF	Impact Force
IIS	Initial Impact Strength
IM	Impact Mass
JFRC	Jute Fiber Reinforced Concrete
$\mathbf{M}_{I3S}$	Impact Moment at the Center of 3-Edge Supported Wall
$\mathbf{M}_{ISS}$	Impact Moment at the Center of Simply Supported Structure

$\mathbf{M}_S$	Static Moment at the Center of Simply Supported Structure
$\mathbf{M}_n$	Nominal Moment Capacity
PC	Plain Concrete
$\mathbf{P}_i$	Impact Load
$\mathbf{P}_{max}$	Maximum Load
$\mathbf{R}_b$	Acceleration Response Recorded on Back of Wall
RC	Reinforced Concrete
$\mathbf{RF}_l$	Longitudinal Resonance Frequency
$\mathbf{RF}_r$	Transverse Resonance Frequency
$\mathbf{RF}_t$	Torsional Resonance Frequency
SCC	Self Compacting Concrete
SEM	Scanning Electron Microscopy
$\mathbf{S}_{max}$	Maximum Spall Extension from the Point of Impact
S-RC	Steel Rebars Reinforced Concrete
S-RC + JF	Steel Rebars Reinforced Concrete having Jute Fibers
$\mathbf{T}_f$	Strength of Fiber Reinforced Concrete in Tension Zone
TI	Toughness Index
UHPC	Ultra-High-Performance Concrete
UHPFRC	Ultra-High-Performance Fiber Reinforced Concrete
UIS	Ultimate Impact Strength

Symbols

β / β'	Coefficient representing the Location of Compression
ε_{cu}	Ultimate Compressive Strain in Concrete
ε_{fu}	Ultimate Tensile Strain of FRP
δ	Strength
ε_o	Strain at Peak Load
Δ	Deformation / Deflection
ξ	Damping Ratio

Chapter 1

Introduction

1.1 Background

Check posts at the entrance of military and strategic facilities are provided to ensure the safety of internal infrastructure and to deal with any outside threat. Therefore, reinforced concrete (RC) walls of these check posts or the internal infrastructure are highly susceptible to experience extreme strain rate loadings due to suicide / grenade explosions [1, 2]. Blast walls are provided worldwide as physical blockades separating valuable assets from explosive threat due to their ability to ensure effective mitigation of blast resultant forces [3]. Performance of concrete against impact loading can be quantified in terms of thickness and pattern of cracks, extent of spalling, strain rate and deflections [4]. Utilization of energy-dissipating methods can aid a structure and its occupants to be protected during a blast [5]. Increase in slab reinforcement ratio specifically at bottom and use of double reinforcement reduces maximum displacement against impact loading [6]. Fibers can be added to enhance static and dynamic properties of concrete to create time lag between impact force and reaction force due to propagation of stress wave [7]. Researchers are using fibers in composites due to their tendency of bearing significant stress and contribution in maintaining concrete strength.

1.2 Research Motivation and Problem Statement

Blast incidents near the check-posts of military structures is an important issue regarding the safety of structures. Concrete walls of check-posts act as a shield for internal buildings as well as for the security personals in case of explosion. These walls may or may not sustain the impact of blast and launch debris. Thus, the performance of reinforced concrete wall needs to be investigated under blast loading. Thus, the problem statement is as follows:

"Impact resistance of normal concrete in terms of toughness against blast loading is a point of concern. Concrete fragments usually lead to severe casualties. Avoiding spreading of concrete fragments due to blast can reduce casualties."

1.3 Overall Goal of the Research Program and Specific Aim of this MS Research

The overall goal of the research program is to replace steel rebars with FRP rebars in concrete structures with additional use of natural fibers for improved durability and performance.

"The specific aim of this MS research work to investigate impact resistance of prototype reinforced concrete walls in laboratory with modified pendulum approach for the effect of jute fibers addition and steel bar replacement with GFRP rebars."

1.4 Scope of Work and Study Limitations

16 walls having different combinations of reinforcing rebars and jute fibers are prepared to conduct impact test. Impact test is divided in to two categories, i.e. low impact and high impact. Each test includes impact testing of walls made up of steel rebars reinforced concrete (S-RC), steel rebars reinforced concrete having

jute fibers (S-RC + JF), GFRP rebars reinforced concrete (GFRP-RC), GFRP rebars reinforced concrete having jute fibers (GFRP-RC + JF). The outcomes of S-RC are taken as reference.

The emphasis of this study is relative comparison. The work is limited to impact testing, investigation of basic dynamic properties (fundamental frequencies and damping ratios), scanning electron microscope (SEM) analysis, empirical modeling and analytical modeling. The other aspects like co-relation of impact mass and prototype mass, analysis of cavities in concrete after casting, durability of jute fiber reinforced concrete and bond between GFRP rebar and concrete are not part of this research.

1.5 Brief Methodology

In this experimental research, mechanical as well as dynamic properties of plain concrete (PC) and jute fiber reinforced concrete (JFRC) are determined. The mix design ratio is 1:2:3:0.6 (cement: sand: aggregate: w/c). 50 mm long jute fibers, 5% by mass of cement are used for preparing JFRC. Walls of size 375 mm × 375 mm × 50 mm are cast and tested for impact resistance and dynamic properties. SEM analysis is performed to examine post-impact fiber concrete bond. Empirical equation has been developed to observe the trend of damping with respect to impact strength. Analytical modeling is done to investigate the moment and impact load capacity of a 3-edge supported wall.

1.6 Thesis Outline

There are six chapters in this thesis, which are as follows:

Chapter 1 consists of introduction, research motivation, problem statement, overall goal, specific aim, scope of work, study limitations, brief methodology and thesis outline.

Chapter 2 contains the literature review. It consists of background, utilization of short discrete natural fibers in concrete for enhanced performance, use of GFRP rebars in concrete structural elements for better durability, prototypes and impact test approaches, novelty of current work and summary.

Chapter 3 contains experimental program. It is divided into background, raw ingredients, mix design and casting technique, properties of PC and JFRC, details of wall specimens and labelling scheme, testing methodology and summary.

Chapter 4 consists of experimental findings. It contains background, impact strength and dynamic response, dynamic properties at different damage stages, SEM analysis for damaged surfaces on JFRC wall specimens and summary

Chapter 5 comprises of discussion. It contains background, empirical modeling for relation between damping and strength at a particular impact, analytical modeling for moment capacity of walls at impact location, utilization of research outcome in real life applications and summary.

Chapter 6 includes conclusion and recommendations.

Bibliography is presented right after chapter 6.

Annexure A includes remaining picture of prototype walls.

Chapter 2

Literature Review

2.1 Background

Impact loading due to events such as blasts create high intensity forces in the form of waves that develops sudden deformation in a structure exposed to it. Blast impact effects the structure using two components. One is the striking of high velocity explosive that results in to damage, the moment it comes in contact to the structure. Second component is the shock wave produced by the blast that create intensified vibrations in the structure. The damage caused can be either small in terms of defragmentation of the material of structure or can be a complete failure of the structure.

2.2 Utilization of Short Discrete Natural Fibers in Concrete for Enhanced Performance

Fibers, as additive act to be crack resistor when randomly distributed in concrete and entirely change the behavior of concrete against static and dynamic loading [8]. Although, concrete performance increases by adding synthetic fibers but they originate from nonrenewable and expensive natural resources [9]. Addition of jute fibers and jute yarns to reinforce cementitious concrete composites contribute in obtaining enriched mechanical results using particular length and content [10]. Jute fibers when added in high-fluidity concrete cause higher improvement in strength as compared to addition in normal concrete [11]. Globally, around 5 % of carbon emissions are due to cement production for industrial activities [12] that categorizes it as worst constituent of concrete for its environmental impact [13]. The addition of fibers by mass of cement in concrete also suggests that by keeping strength value same for both fiber reinforced concrete (FRC) and PC, a noticeable content of cement by weight can be saved [14]. Appropriate content and length of jute fibers reduce the microcracks and porosity of concrete along with delaying cracks initiation and propagation [15]. Greater fiber percentage and length gives higher resistance against projectile impact [16]. Greater fiber content has positive impact on compressive strength of JFRC with increasing curing age [17]. The compressive strength of JFRC decreases as compared to PC against freeze-thaw cycles [18]. The reinforcement design method given in ACI 318-14 [19] neglects the role of concrete in tension zone due to its low contribution. Hussain and Ali [20] used modified form of equation proposed by [21] to incorporate effect of JFRC in tension zone and 50 % of the load difference between PC and JFRC was taken as T_f.

$$M_n = \left[\rho bdfy \times \left(d - \frac{\beta c}{2}\right)\ \right] + T_f\left(\frac{d+c-\beta c}{2}\right) \tag{2.1}$$

2.3 Use of GFRP Rebars in Concrete Structural Elements for Better Durability

Fiber reinforced polymer (FRP) rebars are advantageous due to high strength, lightweight, and non-conductive nature as compared to steel rebars but on the other hand steel rebars for their bending property are preferred when there is a need to provide sufficient anchorage [22]. Post cracking reinforcement strains are higher in GFRP rebars reinforced concrete until failure due to lower axial stiffness

[23]. The bond strength of GFRP rebars embedded in flowable fiber-reinforced engineered cementitious composites is higher as compared to those embedded in normal concrete [24]. Geometrical properties and total mass play major role in resisting dynamic forces. At first contact, inertia forces control resistance under impact loading followed by the contribution of flexural behavior [25]. Rebars contribute towards strength of concrete against impact load by providing resistance in punching deformation. Though, use of GFRP rebars for designing compression members is prohibited by ACI440.1R-15 [26] but the continuous development of strong literature may result in their recommendation for use by international codes in future. ACI 318-14 [19] is not valid for reinforcement design against GFRP rebars. So, moment capacity of concrete reinforced with GFRP rebars can be calculated by using the formula given in [26].

$$M_n = A_f f_{fu} \times \left(d - \frac{\beta_1 c_b}{2}\right) \tag{2.2}$$

Where c_b is the depth of compression zone at balanced strain condition; calculated as

$$c_b = \frac{\varepsilon_{cu} \times d}{\varepsilon_{cu} + \varepsilon_{fu}}$$

Ejaz and Ali [27] combined the effect of JFRC reinforced with GFRP rebars and proposed an equation to calculate moment capacity and 53 % of the load difference between PC and JFRC was taken as T_f.

$$M_n = A_f f_{fu} \times \left(d - \frac{\beta_1 c_b}{2}\right) + T_f\left(\frac{d + c - \beta c}{2}\right) \tag{2.3}$$

2.4 Prototypes and Impact Test Approaches

Experimental investigations on FRC conducted by previous researchers consist of full-scale testing, scaled down prototype testing and testing with relative approach.

Table 2.1 shows different prototype testing approaches utilized by researchers to investigate the impact resistance of FRC. Li et al. [28] used bullet projectile impact to investigate the penetration depth and damage patterns in ultra-high-performance fiber reinforced concrete (UHPFRC) disks. Hussain and Ali [20] applied the free-falling drop weight approach to investigate the impact strength of JFRC slabs. Liu et al. [29] used cartridge projectile impact to investigate the crater diameter, volume loss and penetration depth of ultra-high-performance concrete (UHPC) cylinders. Wang and Chouw [30] utilized instrumented drop weight mechanism to investigate the flexural behavior of coconut fiber reinforced concrete (CFRC) beams under impact loading. Mastali et al. [31] utilized the instrumented drop weight mechanism to investigate the impact strength of self-compacting concrete cylinders having recycled GFRP.

Table 2.1: Previous impact test mechanisms on prototypes.

Reference	Impact Mechanism	Impact Weight / Velocity	Prototype Specifications	Outcome
Li et al. [28]	Bullet Projectile Impact	843 and 926 m/s	UHPFRC Disks 120 x 300 mm	Penetration Depth and Damage Patterns
Hussain and Ali [20]	Free Falling Drop-Weight	1.25 kg	JFRC Slabs 430 x 280 x 75 mm	Impact Strength (No. of Blows)
Liu et al. [29]	Cartridge Projectile Impact	550 and 800 m/s	UHPC Cylinders 750 x 700 mm	Crater Diameter, Volume Loss and Penetration Depth
Wang and Chouw [30]	Instrumented Drop Weight	48 kg	CFRC Beams 100 x 100 x 500 mm	Force-time History, Energy Absorption
Mastali et al. [31]	Instrumented Drop Weight	4.45 kg	GFRP SCC Cylinders 150 x 65 mm	Impact Strength (No. of Blows)

Pham and Hao [32] proposed resultant moment and shear force against maximum impact force for a flexural member and suggested that if a member experiences flexural damage due to static loading then it is most likely that the member will experience shear damage due to impact loading. In case of zero overhang, the peak dynamic bending moment will be three times smaller than static bending moment. Figure 2.1 shows the BMD under static load and impact load for simply supported structure.

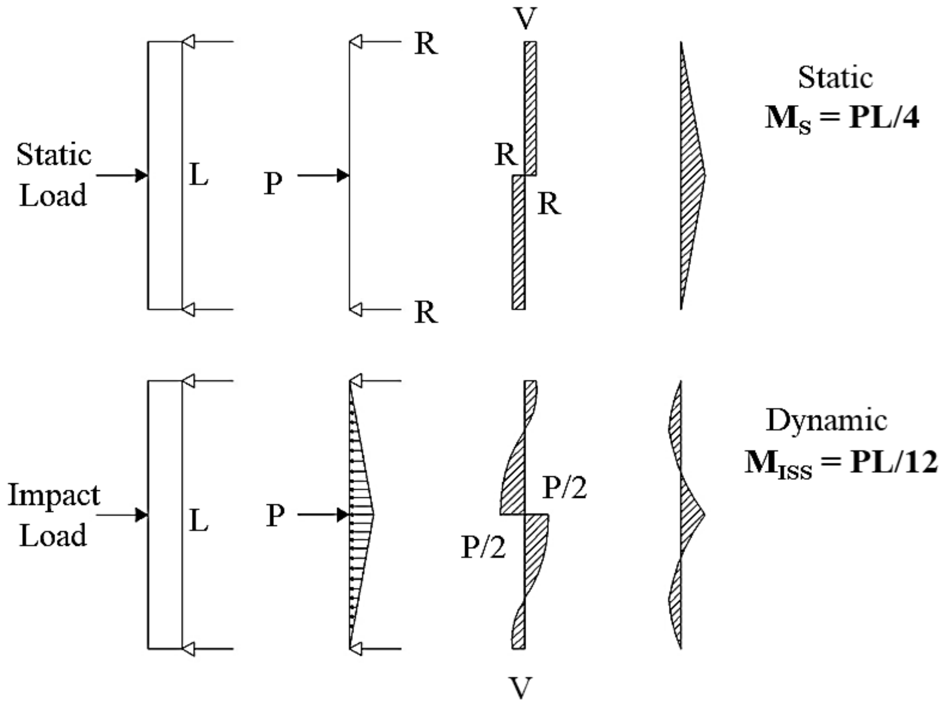

FIGURE 2.1: BMD under static load and impact load for simply supported structure Pham and Hao [32].

2.5 Novelty of Current Work

ACI 544.2R-89 [33] describes two types of impact test approaches based on kinetic energy as shown in Figure 2.2. One is instrumented drop weight test and other is pendulum type charpy's impact test. Both approaches estimate the sum of repetition of blows to have a quantitative evaluation of the energy absorbed by structure. This approach is advantageous for relative comparison between the specimens of normal concrete and FRC.

To the best of scholar's knowledge, no work has been done to investigate the impact resistance of RC walls having jute fibers and GFRP rebars using pendulum impact approach. Therefore, this study helps to understand behavior of RC walls reinforced with jute fibers and GFRP rebars for possible application against impact loading.

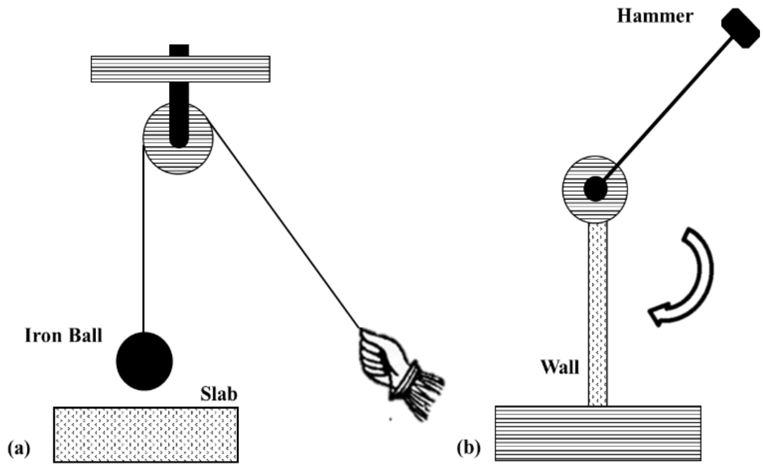

FIGURE 2.2: Simplified impact test approaches Ahmed and Ali [34].

2.6 Summary

Impact resistance investigation using state of the art equipment gives output at a higher accuracy level as compared to simplified prototype testing. The behavior of concrete against impact loading can be predicted better by conducting the full scale blast testing in field as well as laboratories. Empirical modeling can be used to develop relations in order to perform simplified testing with the identification of error percentages. GFRP rebars as replacement of steel rebars give more or less same results with the advantage of GFRP rebars being light weight and corrosion resistant. Literature supports the inclusion of artificial fibers in improving the impact resistance of concrete. Use of natural fibers in optimum percentage can play a vital role in enhancement of impact strength of concrete.

Chapter 3

Experimental Program

3.1 Background

In case of an air blast, bearing balls disperse and strike with high velocity at near structures due to excitation in arbitrary directions. This phenomenon causes damage of structures leading to breakup and launch of debris as shown in Figure 3.1. Ability of RC structures to sustain extreme dynamic loading greatly depends upon dynamic response characteristics, scattering pattern and flight range of debris [35, 36].

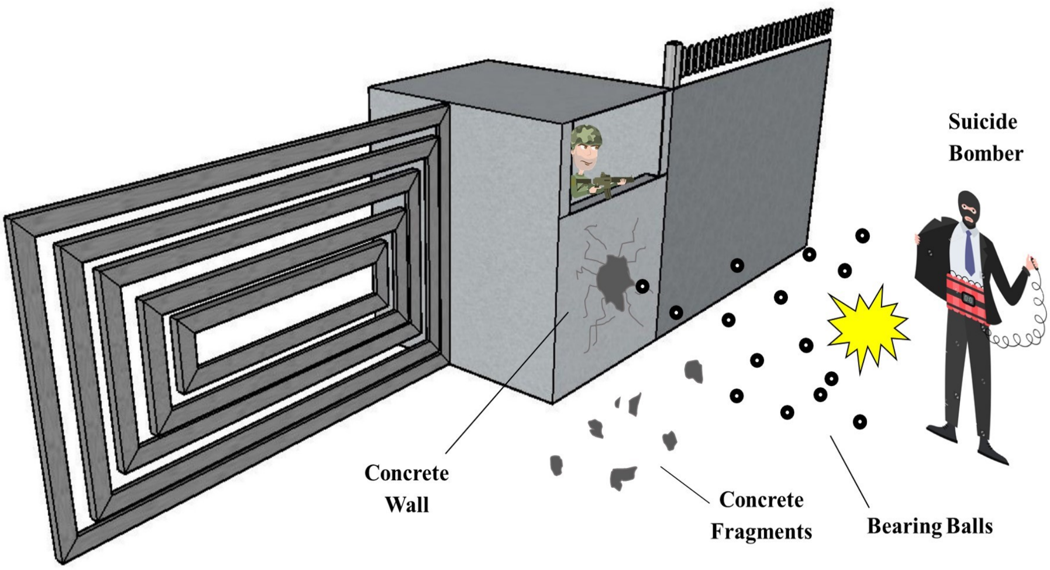

FIGURE 3.1: Probable scenario of blast near a security check post.

Fibers not only enhance energy absorption capacity of concrete but also increase post-failure residual strength. GFRP rebars due to their non-corrosive property are considered as a better solution instead of steel rebars to resist in a moist environment. The use of jute fibres as additives along with GFRP rebars as reinforcement is explored against impact loading through experimental evaluation. In this chapter raw ingredients, mix design and casting technique, mechanical properties along with basic dynamic properties and SEM analysis, wall specimens and testing methodology are explained in detail.

3.2 Raw Ingredients

Locally available materials including ordinary portland cement, lawrencepur sand, 12.5 mm down coarse aggregates and water are used to prepare PC. To start with, jute fiber has been selected due to its local availability. To prepare JFRC, same ingredients are used with jute fibers. Table 3.1 shows the mechanical properties of jute fibers reported by [37]. Jute fibers in raw form are first cut in to lengths of 50 mm and then soaked into water for 24 hours. Raw fibers, prepared fibers and fiber cut length is shown in Figure 3.2a, 3.2b and 3.2c, respectively. To study the resistance of fiber against tensile failure in terms of fiber pull-out and fiber breakage, fiber length is taken as 50 mm based on assumption that hypothetically half the length of fiber will remain embedded when concrete will undergo ultimate failure and spall up to 25 mm. SEM analysis is conducted to study the outer surface condition of fiber. Figure 3.2d shows the micro-structure of jute fibers comprising of nano strands with diameter ranging from 39.60 um to 61.86 um. Figure 3.2e shows the fiber end which contains swelled tubular strand edges due to enough water absorption. Steel rebars and GFRP rebars having length 350 mm and diameter 6 mm are used as reinforcement as shown in Figure 3.3a. The relative behavior of both rebars against tensile strength test is shown in Figure 3.3b. The tensile strength of Steel rebar and GFRP rebar came out to be 537.6 MPa and 756.94 MPa, respectively.

TABLE 3.1: Mechanical properties of jute fibres [37].

Properties	Values
Length (mm)	1.5-120
Diameter (um)	20-200
Density (kg/m^3)	1300-1490
Tensile Strength (MPa)	320-800
Tensile Modulus (GPa)	8-78
Max. Elongation (%)	1-1.8

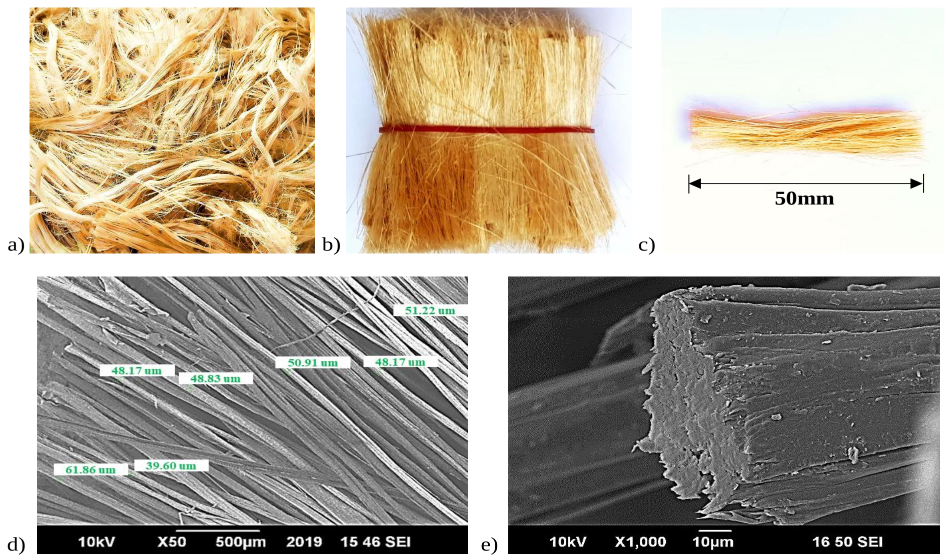

FIGURE 3.2: Jute fibers; a) raw fibers, b) prepared fibers, c) fiber cut length, d) 500m SEM view, e) fiber end.

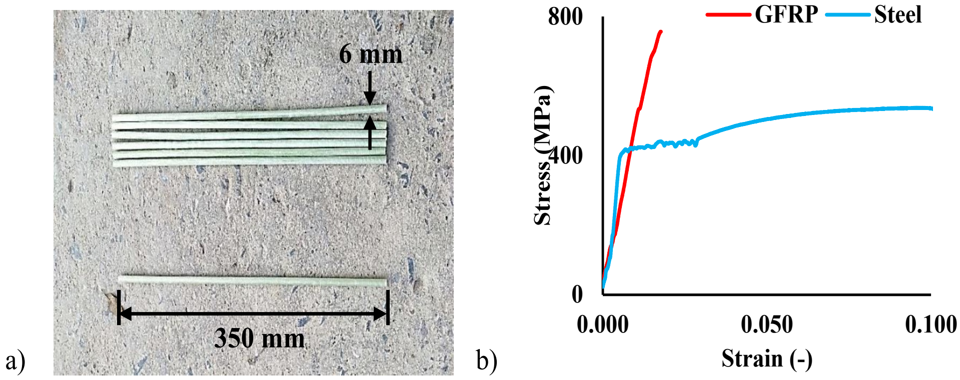

FIGURE 3.3: GFRP rebars; a) naked eye view, b) relative tensile strength of steel and GFRP rebar.

3.3 Concrete Preparation

3.3.1 Mix Design

For the preparation of PC, 1:2:3 (Cement: Sand: Aggregate) mix design ratio is used with water cement ratio 0.6. For the preparation of JFRC same ratio along with 50 mm long jute fibers, 5% by mass of cement are used. Mix design is kept same for both PC and JFRC expect further addition of water to make JFRC workable due to high water absorption of jute fibers. In addition, the workable mix is properly compacted to obtain good strength. The actual w/c ratio of JFRC is referred optimum as further water addition would have caused bleeding. The same concept was utilized by [38] to prepare CFRC. In this study, dosage of jute fibers is purposely linked with mass of cement in context of binding characteristics between fibers and concrete matrix. Agricultural waste fibers of plants with greater pozzolanic reactivity have been widely used by researchers as partial cement replacement due to consumption of high quantity of minerals and silicates from earth during their growth [39]. Fiber length, fiber content and water cement ratio have been selected keeping in view previous literature on FRC [40–42] to achieve enhanced energy absorption and toughness index. The target strength against selected mix design is taken 15 MPa. The reason for taking this target strength is to make the structure economical with the aim of achieving the high energy absorption because in case of impact loading at small structures (single story check posts) high compressive strength is not necessary rather high energy absorption is beneficial. So, instead of providing expensive blast walls in developing countries, concrete walls having minimum required compressive strength with high energy absorption can be an economical solution.

3.3.2 Casting Technique

Dry constituents are added in layers. Firstly, a layer of one third proportion of coarse aggregates, then a layer of fibres are added in the mixer. The next layer of one third fine aggregates is placed and above that a layer of fibres is laid. After placing another set of these layers, the mixer is rotated for 4 minutes during which two third of water is added after rotation of 3 minutes. After that rest of the dry material is added in same layering strategy and mixer is rotated for 2 minutes while adding remaining water. Slump test is performed as per specifications of ASTM C143 [43] to examine the workability of PC and JFRC which came out to be 58 mm and 36 mm respectively. For determining the mechanical properties, cylinders of size 100 mm x 200 mm and beamlets of size 100 mm x 100 mm x 450 mm are filled by adopting the standard procedure of filling in three layers and tamping each layer 25 times using a standard tamping rod. The specimens are kept in water for 28 days and then dynamic testing is performed as per ASTM C215 [44].

3.3.3 Properties of PC and JFRC

TABLE 3.2: Dynamic results of cylinders and beamlets.

Specimen		RF_l (Hz)	RF_t (Hz)	RF_r (Hz)	Damping (%)
(1)	(2)	(3)	(4)	(5)	(6)
Cylinder	PC	2809.2 ± 741.8	1509 ± 0	3003.4 ± 835.6	4.7 ± 0.9
	JFRC	1952.8 ± 887.7	1334.8 ± 652.7	1486.9 ± 954.3	6.2 ± 1.3
Beamlet	PC	2248.3 ± 1346.7	3121.7 ±1139.3	3195.7 ±799.3	2.8 ± 0.8
	JFRC	1227.7 ± 103.3	1488 ± 446	1242.3 ± 88.7	3.5 ± 0.3

The results of dynamic testing are shown in Table 3.2. It can be seen that damping ratio of JFRC cylinder is 6.2 which is 32% more than the 4.7 damping ratio of PC cylinder. Similarly, the damping ratio of JFRC beamlet is 3.5 which is 25% more than the 2.8 damping ratio of PC beamlet.

TABLE 3.3: Mechanical properties of PC and JFRC under compression, splitting-tension and flexure.

Property	Specimen	P_{max} (kN)	δ (MPa)	ε_o (-)	Δ (mm)	E_α (-)		E_β (-)		E_T (-)		TI (-)
(1)	(2)	(3)	(4)	(5)	(6)	(7)		(8)		(9)		(10)
Compression	PC	101.41 $\pm$ 12.45	14.66 $\pm$ 1.55	0.0141 $\pm$ 0.007	-	0.057 $\pm$ 0.007	MJ/m^3	0.121 $\pm$ 0.003	MJ/m^3	0.178 $\pm$ 0.010	MJ/m^3	3.11 $\pm$ 0.19
	JFRC	92.13 $\pm$ 16.05	11.33 $\pm$ 1.95	0.0707 $\pm$ 0.055	-	0.082 $\pm$ 0.006	MJ/m^3	0.195 $\pm$ 0.016	MJ/m^3	0.277 $\pm$ 0.021	MJ/m^3	3.38 $\pm$ 0.03
Splitting - tension	PC	70.45 $\pm$ 6.9	8.69 $\pm$ 0.85	-	1.88 $\pm$ 0.33	17.00 $\pm$ 3.88	J	0	J	17.00 $\pm$ 3.88	J	1 $\pm$ 0
	JFRC	48.14 $\pm$ 6.85	5.94 $\pm$ 0.85	-	0.91 $\pm$ 0.41	20.04 $\pm$ 3.48	J	29.49 $\pm$ 4.67	J	49.53 $\pm$ 8.15	J	2.47 $\pm$ 0.13
Flexure	PC	12.06 $\pm$ 0.25	4.23 $\pm$ 0.01	-	1.695 $\pm$ 0.2	6.36 $\pm$ 0.25	J	0	J	6.36 $\pm$ 0.25	J	1 $\pm$ 0
	JFRC	6.84 $\pm$ 0.25	2.3 $\pm$ 0.2	-	1.33 $\pm$ 0.04	4.36 $\pm$ 0.26	J	9.16 $\pm$ 1.13	J	13.52 $\pm$ 1.39	J	3.10 $\pm$ 0.13

The specimens are then tested in servo-hydraulic testing machine to investigate compression, splitting tension and flexural strengths as per ASTM standards C39 [45], C496 [46], C78 [47] using the average of ranges given for loading rates. Table 3.3 shows the results of different parameters obtained from mechanical testing of cylinders and beamlets. The strength of JFRC under compression is 11.33 MPa and that of PC is 14.66 MPa that shows a 22.7% decrement in compressive strength. But, the strain at peak load of JFRC came out to be 0.0707 that is 401.5% greater than 0.0141 strain of PC. The energy absorption of uncracked specimen of JFRC is 0.082 MJ/m3 that is 43.9% greater than 0.057 MJ/m3 of PC. Similarly, the energy absorption of JFRC after maximum load is 0.195 MJ/m3 that is 61.2% greater than 0.121 MJ/m3of PC. The toughness index of JFRC is 3.38 as compared to 3.11 of PC. The strength of JFRC under splitting-tension is 5.94 MPa that is 31.65% less than 8.69 MPa strength of PC. The deformation of JFRC at peak load is 0.91 mm that is 51.6% less than 1.88 mm deformation of PC. Energy absorption of uncracked JFRC specimen is 20.04 J that is 17.8% greater than 17.00 J of PC. Total Energy absorption of JFRC after maximum load is 49.53 J that is 191.4% greater than 17.00 J of PC. The toughness index of JFRC is 2.47 as compared to 1 of PC. The strength of JFRC under flexural loading is 2.3 MPa that is 45.6% less than 4.23 MPa strength of PC. The deflection of JFRC at peak load is 1.33 mm that is 21.53% less than 1.695 mm deflection of PC. Energy absorption of uncracked JFRC specimen is 4.36 J that is 31.45% less than 6.36 J of PC. Total Energy absorption of JFRC after maximum load is 13.52 J that is 112.6% greater than 6.36 J of PC. The toughness index of JFRC is 3.10 as compared to 1 of PC. The greater toughness index of JFRC than PC under compression, splitting-tension and flexure shows the better post crack energy absorption capacity. Figure 3.4a shows the development of cracks and stress strain curve displaying the behavior of PC and JFRC cylinder under compression. The loading rate applied is 0.25 MPa/sec. It can be seen that first crack appeared in PC is smaller than that of JFRC whereas at maximum load the cracks are larger and more in PC than in JFRC. At ultimate load, a significant portion of concrete is experienced spalling out in PC due to brittleness, however in JFRC there is only widening of cracks. This shows the effectiveness of jute fibers in restricting the concrete from spalling out due to existence of bridging effect created by fibers. The stress strain curve shows that the maximum load attained by JFRC is at a higher strain than PC. SEM image shows the fiber concrete condition specifically at a location of JFRC cylinder where a significant part of concrete is bulged out due to compressive loading. The fibers showed resistance and held the concrete from spalling and a pull-out phenomenon of fiber from concrete matrix is observed that damaged the outer surface of fiber.

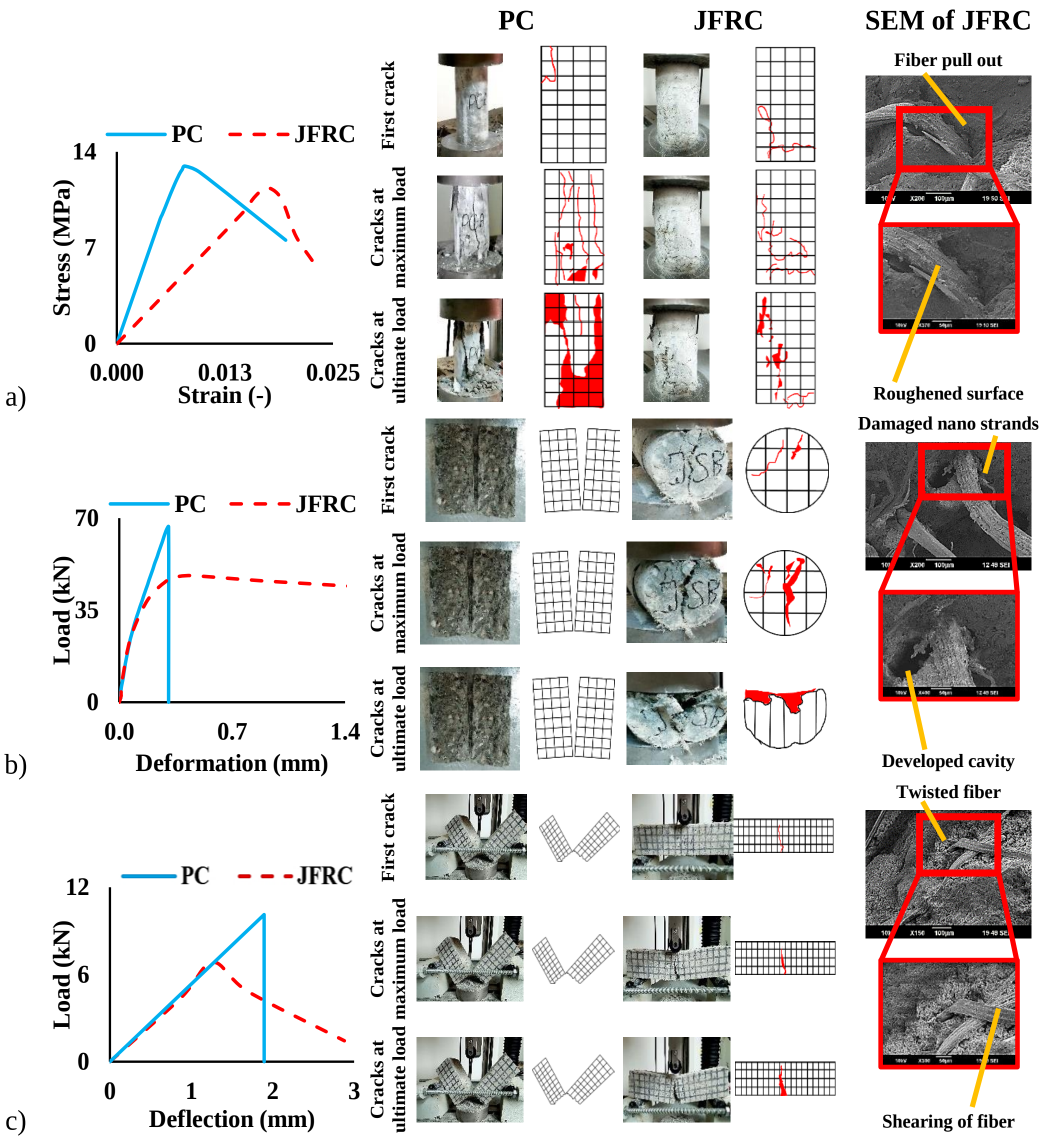

FIGURE 3.4: Mechanical behavior, cracking patterns and SEM analysis; a) compression, b) split-tension and c) flexure.

Also, as the concrete bulged out, the fiber got twisted without the disintegration of nano strands that shows the better elastic behavior of fiber. Figure 3.4b shows the failure pattern and load deformation curve of PC and JFRC cylinder under splitting tension. The loading rate applied is 1.05 MPa/min. It can be seen that PC cylinder split in to half at maximum load without any initial cracking. Whereas the JFRC cylinder showed minor initial cracking then widening of those cracks at maximum load. But JFRC cylinder showed almost splitting in to half at ultimate load. The load deformation curve shows the load carrying capacity of PC almost double than JFRC. However, it can be seen that after reaching the maximum loading stage JFRC has taken enough load due to the combination of fiber concrete bond and tensile strength of fiber SEM image shows the fiber concrete condition specifically at the location of JFRC cylinder where specimen divided in two halves due to splitting-tensile load. It is clearly evident from the fiber condition that fiber showed resistance to splitting of concrete due to which the nano strands of fiber were damaged severely. A cavity is created around the fiber due to pull-out in the opposite direction. Figure 3.4c shows the load deformation curve and failure of PC and JFRC beamlets under thrird-point flexural loading. The loading rate applied is 1.035 MPa/min. PC beamlet failed at maximum load and divided in to two halves without showing initial cracks. JFRC beamlet showed a hair line crack starting from the bottom center. At maximum load the crack widened and at ultimate load the beamlet almost divided into two parts. The load deformation curve shows the complete failure of PC after maximum load. The JFRC has taken significant load after reaching the maximum load which shows the resistance of beamlet against division in two halves. SEM image shows the fiber concrete condition at the location from where the bottom mid portion of JFRC beamlet started to deflect and then divided in two halves. The fiber remained embedded in concrete matrix and twisted gradually due to deflection. The concrete separated apart and fiber got pulled out.

3.4 Wall Specimens and Labelling Scheme

Figure 3.5 shows the scaling down of approximately 1/6 to create a prototype wall panel against front wall of check post. Simplified boundary conditions show a 3-edge supported wall panel. Prototype walls of size 375 mm x 375 mm x 50 mm are prepared to conduct impact tests. Visually, no cavities are noticed in concrete after casting.

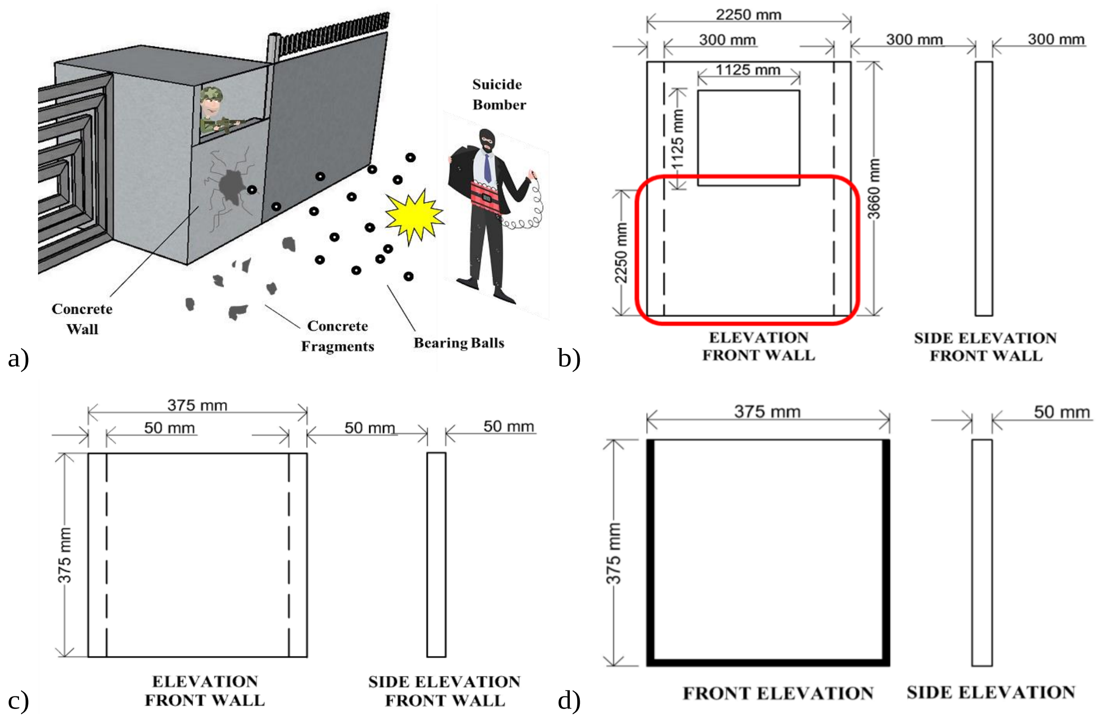

FIGURE 3.5: Scaling down-simplified approach; a) probable scenario of blast, b) schematic diagram of front wall of check post, c) scaled down region, d) simplified boundary condition.

Impact tests are divided in to two categories, i.e. low impact and high impact. For both categories, two walls each are prepared for all four combinations of fiber and reinforcement in concrete, i.e. steel rebars reinforced concrete wall, steel rebars reinforced concrete wall having jute fibers, GFRP rebars reinforced concrete wall, GFRP rebars reinforced concrete wall having jute fibers. The details of walls prepared and their labelling is shown in Table 3.4. A mesh of 6 x 6 rebars is provided in each wall with varying spacing to create a reinforcement cell size of

75 mm by 75 mm at the center where the impact load is supposed to act. The reinforcement plan of walls prepared is shown in Figure 3.6.

TABLE 3.4: Labelling scheme of wall panels.

Test Variable	Impact Weight	PC	JFRC
(1)	(2)	(3)	(4)
Low Impact	2.215 kg	S-RC 3	S-RC + JF 1
	2.215 kg	S-RC 4	S-RC + JF 2
	2.215 kg	GFRP-RC 1	GFRP-RC + JF 1
	2.215 kg	GFRP-RC 2	GFRP-RC + JF 2
High Impact	2.925 kg	S-RC 1	S-RC + JF 3
	2.925 kg	S-RC 2	S-RC + JF 4
	2.925 kg	GFRP-RC 3	GFRP-RC + JF 3
	2.925 kg	GFRP-RC 4	GFRP-RC + JF 4

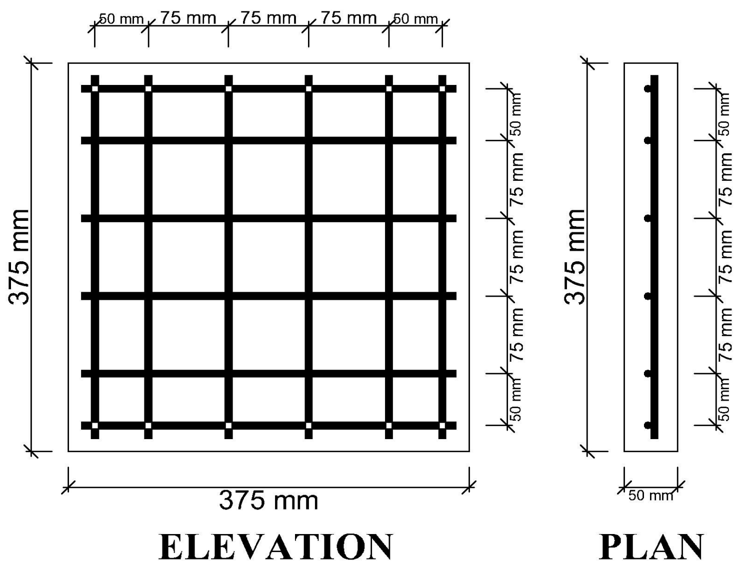

FIGURE 3.6: Wall reinforcement plan.

3.5 Testing

3.5.1 Modified Pendulum (Impact) Test Setup

Real blast conditions vary with parameters like distance and weight of explosives. Its replication requires limitless resources and professional expertise from other related specialties. This study is based on relative approach with the emphasis on the effectiveness of fibers addition and rebar replacement against impact loading. In a blast incident, blast pressure is generated and at the centroid maximum load is employed. Figure 3.7 shows the schematic visualization of blast components.

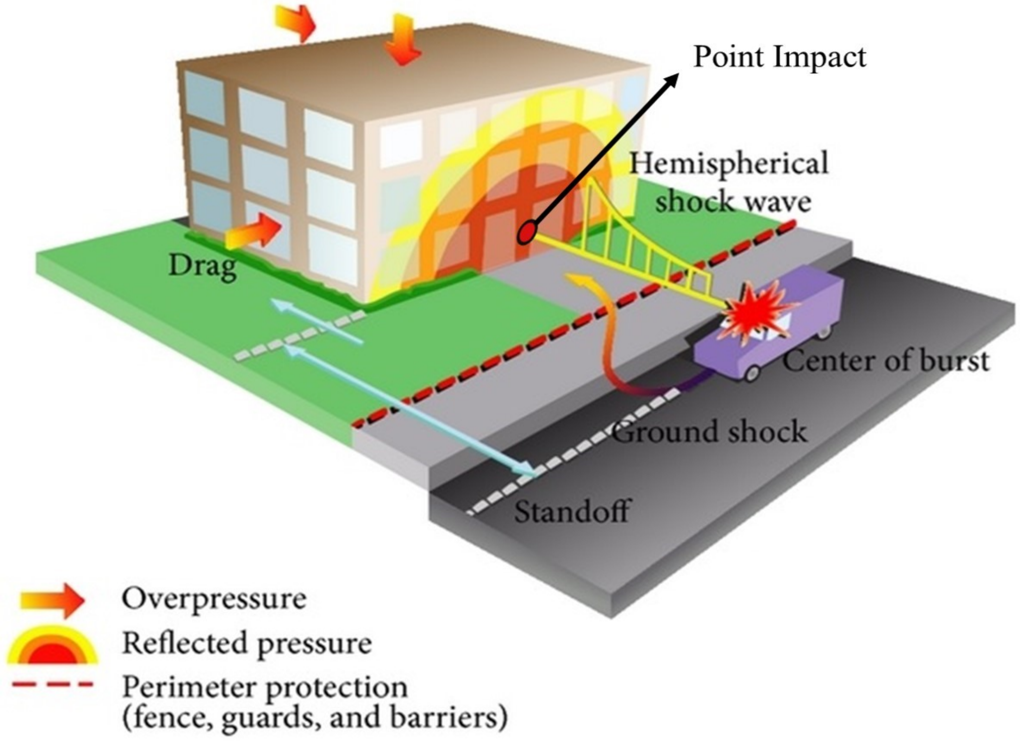

FIGURE 3.7: Schematic visualization of blast components Yalciner [48].

Impact testing is performed using modified pendulum impact apparatus developed to co-relate the effect of that particular point impact on a 3-edge supported wall panel. Edge restraints at three sides of wall are shown in Figure 3.8. The hammer can be released from any angle having a certain angular distance e.g. 30^o, 60^o and 90^o to apply the impact covering the angular distance of 32 cm, 64 cm and 96 cm, respectively, before striking the specimen. Two impact weights are used in this test, i.e. 2.215 kg and 2.925 kg based on which the relative terms are assigned as low impact and high impact. The values of weight are kept close to analyze the damaging effect of small increment of impact load. These values contain weight of hammer as well as weight of arm that's why the value of weight is taken up to three decimal places. ACI 544.2R-89 [33] states that impact resistance can be measured by the number of strikes in a re-peated impact test to achieve a prescribed level of distress and this concept has been utilized by [20, 31]. So, the unit of impact strength is taken as the number of strikes.

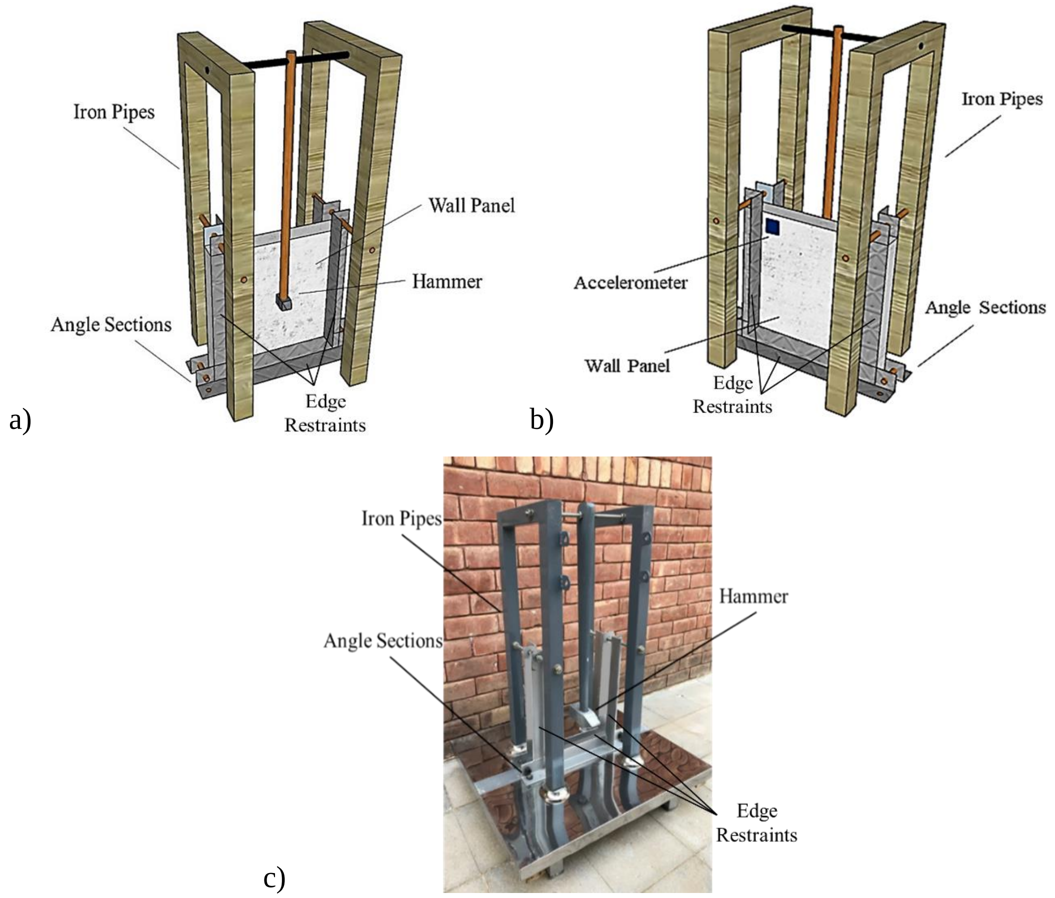

Figure 3.8: Impact testing mechanism; a) impact location, b) accelerometer location, c) test set up.

Hussain and Ali [20] used an impact weight of 1.25 kg dropped from 60 cm and 90 cm heights. In this study, two hammers of impact weight (2.215 kg and 2.925 kg) are released from 90^o angle to generate impact covering an angular distance of 96 cm till development of initial cracking and ultimate failure (The specimen is said to be failed when the spall depth of concrete reaches to 25 mm). The out-comes of S-RC are taken as reference. During impact testing, accelerometers are used to record acceleration-time graphs of hammer strikes and their response at the back face of wall 50 mm far from the top right corner. Figure 3.8a and 3.8b shows the location of impact strikes and location of mounted accelerometer, respectively.The accelerometers mounted on hammer and the back side of the wall recorded the acceleration time history of every impact on the wall. The data was extracted using MATLAB program and then filtered using SeismoMatch 2018 to have a pure response of wall against impact.

3.5.2 Determination of Dynamic Properties at Different Damage Stages

Dynamic testing is performed before impact test, after initial impact strength failure (IIS), and after ultimate impact strength failure (UIS) as per specifications of ASTM C 215 [44]. Only basic dynamic properties (fundamental frequencies and damping ratios) are calculated. Detailed investigation of damping characterization is beyond the scope of this study. Figure 3.9 shows the location of accelerometer and hammer strikes for obtaining respective frequencies.

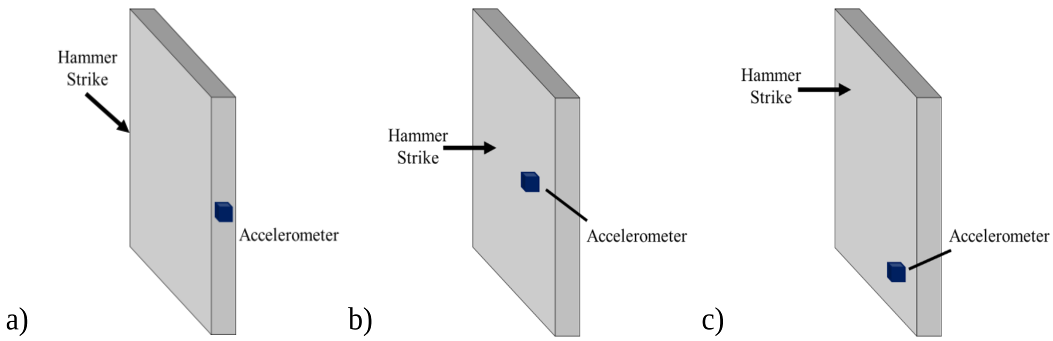

FIGURE 3.9: Dynamic testing mechanism as per ASTM C 215 [44]; a) for longitudinal frequency, b) for transverse frequency, c) for rotational frequency.

3.5.3 Scanning Electron Microscopy of Damaged Surfaces on JFRC Wall Specimens

SEM analysis is performed on damaged surface of JFRC after being transported to testing facility without any further deterioration to analyze the effect of hammer strikes on fiber surface and post impact fiber concrete bond.

3.6 Summary

Concrete is prepared with mix design ratio of 1:2:3 (Cement: Sand: Aggregate) and jute fibers, 5% by mass of cement. Water cement ratio is taken 0.6. Mechanical properties show that cracked energy absorption is more in JFRC along with greater damping than PC. SEM analysis indicated good performance of concrete fiber bond and resistance of fiber against tension. Based on these properties a total of 16 walls are prepared having steel and GFRP reinforcement bars of diameter of 6 mm to conduct impact tests.

Chapter 4

Experimental Findings

4.1 Background

Wall Specimens are prepared with the mix design ratio of 1:2:3 (Cement: Sand: Aggregate) and jute fibers, 5% by mass of cement. Water cement ratio is taken 0.6. 16 walls are prepared having combination of jute Fibers with steel and GFRP reinforcement bars of diameter of 6 mm. Impact testing results, basic dynamic properties results and SEM analysis of walls are discussed in this chapter.

4.2 Impact Strength and Dynamic Response

4.2.1 Initial and Ultimate Impact Strength of Walls

The results of wall panels tested against low impact and high impact are shown in Table 4.1. The initial strength of S-RC wall against low impact came out to be 34.5 strikes and ultimate strength came out to be 110.5 strikes. However, initial strength of S-RC wall having jute fibers against low impact came out to be 60.5 strikes and ultimate strength came out to be 149 strikes. The maximum spall distribution in either direction from the point of impact came out to be 71.6 mm for S-RC wall which is less than 78.1 mm of S-RC wall with jute fibers. Similarly, initial strength of GFRP-RC wall against low impact came out to be 32.5 strikes and ultimate strength came out to be 54 strikes. However, initial strength of GFRP-RC wall having jute fibers against low impact came out to be 72.5 strikes and ultimate strength came out to be 163 strikes. The maximum spall distribution in either direction from the point of impact came out to be 81.8 mm for GFRP-RC wall which is more than 71.9 mm of GFRP-RC wall with jute fibers.

TABLE 4.1: Impact strength parameters

Specimen Type	IM (kg)	IF (N)	IIS (strikes)	UIS (strikes)	S_{max} (mm)
(1)	(2)	(3)	(4)	(5)	(6)
S-RC	2.215	5.02	34.5 ± 10.5	110.5 ± 4.5	71.6 ± 9.6
S-RC + JF	2.215	5.10	60.5 ± 1.5	149 ± 7	78.1 ± 15.6
GFRP-RC	2.215	5.10	32.5 ± 10.5	54 ± 21	81.8 ± 7
GFRP-RC + JF	2.215	4.98	72.5 ± 11.5	163 ± 13	71.9 ± 3.1
S-RC	2.925	6.74	33.5 ± 2.5	48.5 ± 0.5	70.9 ± 11.6
S-RC + JF	2.925	6.78	46.5 ± 4.5	123.5 ± 17.5	74.1 ± 4.1
GFRP-RC	2.925	6.64	32 ± 1	57.5 ± 4.5	71.3 ± 10
GFRP-RC + JF	2.925	6.85	53 ± 8	148 ± 20	56.9 ± 11.9

The initial strength of S-RC wall against high impact came out to be 33.5 strikes and ultimate strength came out to be 48.5 strikes. However, initial strength of S-RC wall having jute fibers against high impact came out to be 46.5 strikes and ultimate strength came out to be 123.5 strikes. The maximum spall distribution in either direction from the point of impact came out to be 70.9 mm for S-RC wall that is slightly less than 74.1 mm of S-RC wall with jute fibers. Similarly, initial strength of GFRP-RC wall against high impact came out to be 32 strikes and ultimate strength came out to be 57.5 strikes. However, initial strength of GFRP-RC wall having jute fibers against high impact came out to be 53 strikes and ultimate strength came out to be 148 strikes. The maximum spall distribution in either direction from the point of impact came out to be 71.3 mm for GFRP-RC wall which is significantly greater than 56.9 mm of GFRP-RC wall with jute fibers.

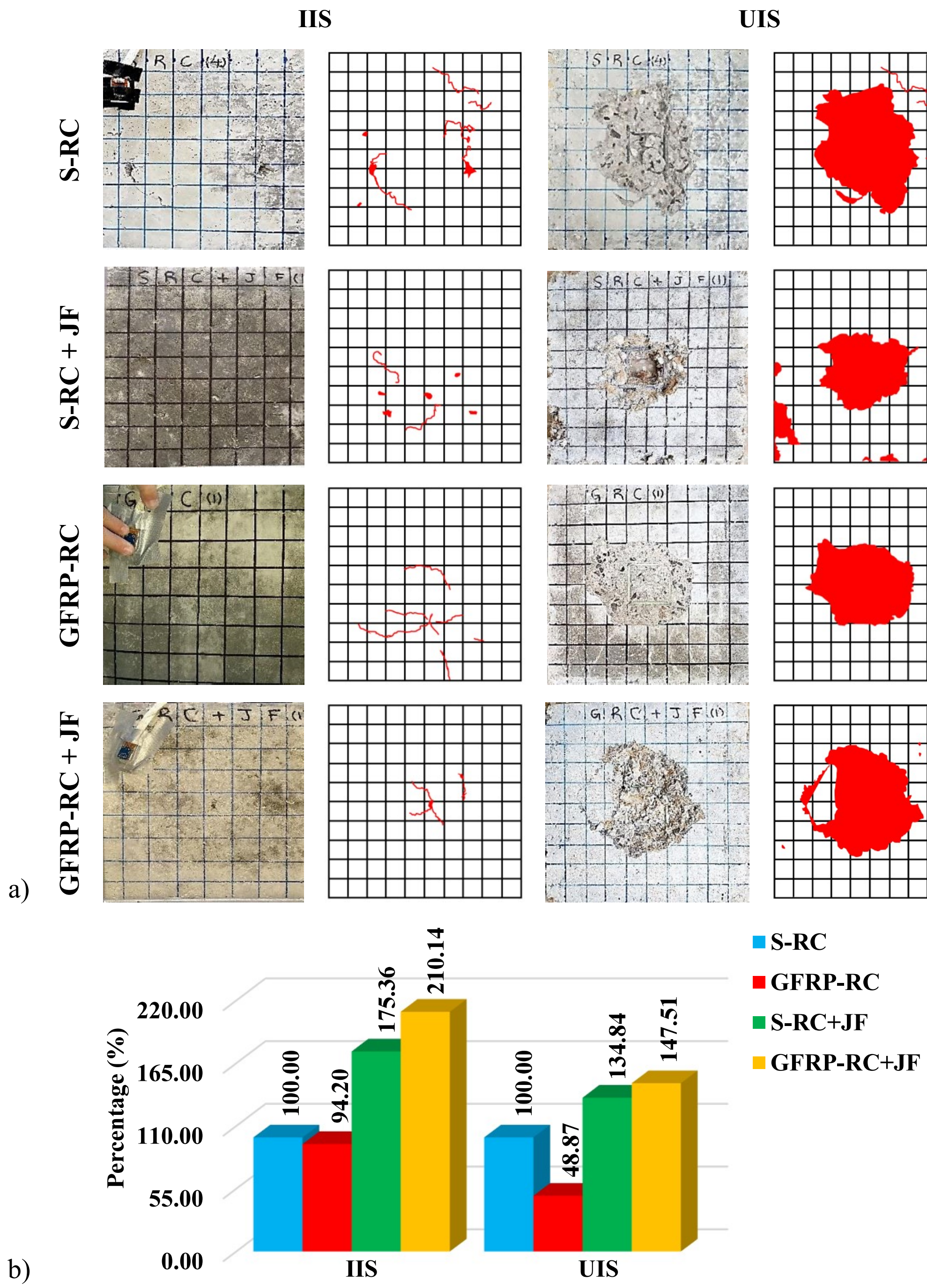

FIGURE 4.1: Impact testing results of low impact; a) cracking patterns, b) impact strength percentages.

Figure 4.1a shows the cracking behavior of walls against low impact. Schematic diagrams are used to have a clear understanding of the generation of cracks and their outward propagation. Figure 4.1b shows the comparison of impact strength percentages of walls. The outcome of S-RC is assigned a reference value 100% with respect to which results of other combinations are reported in terms of percentage increment and decrement. It can be perceived that IIS of GFRP-RC has decreased to 94.2%. However, IIS of S-RC having jute fibers and GFRP-RC having jute fibers has increased to 175.36% and 210.14%, respectively. Similarly, UIS of GFRP-RC has decreased to 48.87% and UIS of S-RC having jute fibers and GFRP-RC having jute fibers has increased to 134.84% and 147.51%, respectively.

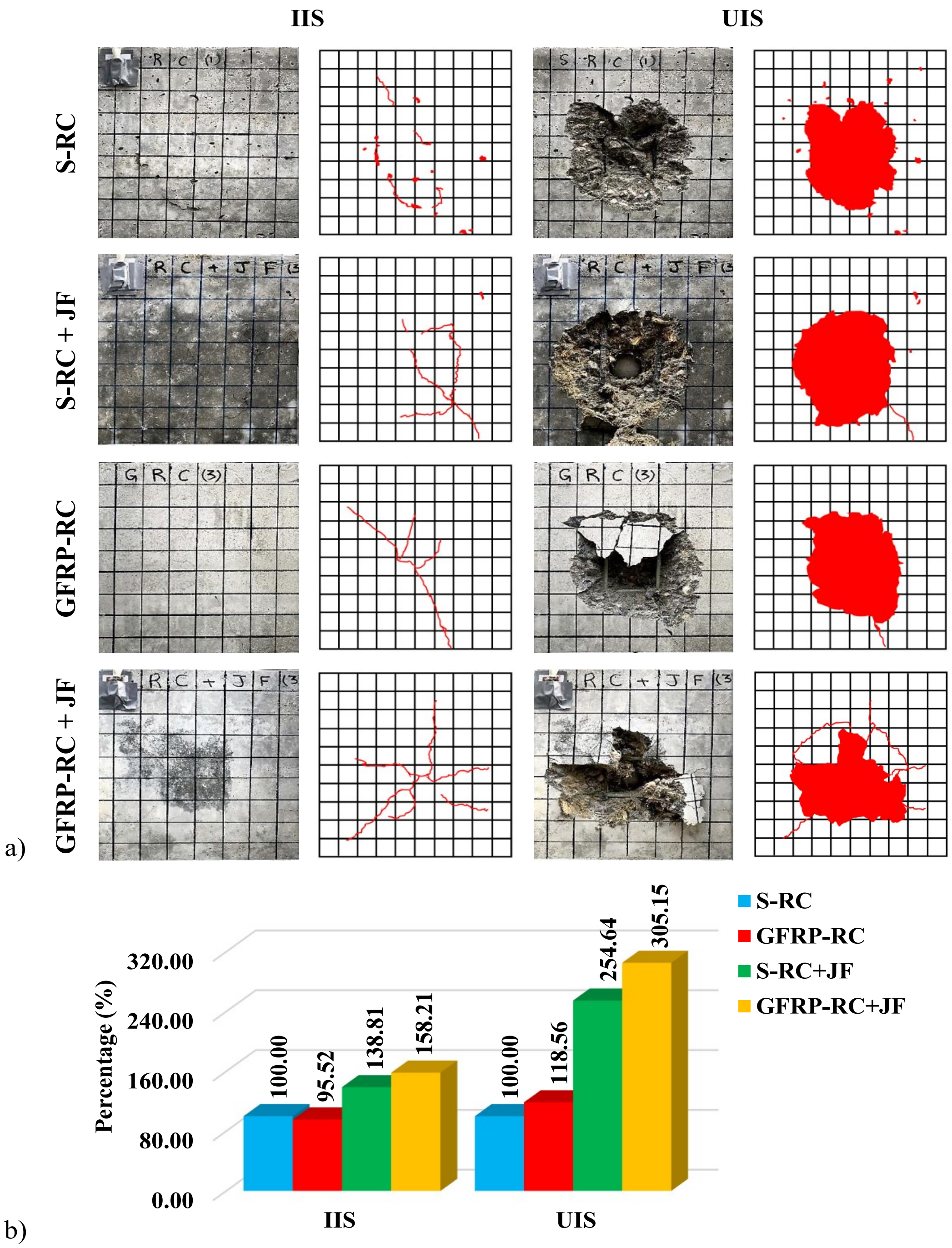

FIGURE 4.2: Impact testing results of high impact; a) cracking patterns, b) impact strength percentages.

Figure 4.2a shows the cracking behavior of walls against high impact. Schematic diagrams show the generation of cracks and their outward propagation. Figure 4.2b shows the comparison of impact strength percentages of walls. The outcome of S-RC is assigned a reference value 100% with respect to which results of other combinations are reported in terms of percentage increment and decrement. It can be seen that IIS of GFRP-RC has decreased to 95.52%. However, IIS of S-RC having jute fibers and GFRP-RC having jute fibers has increased to 138.81% and 158.21%, respectively. Similarly, UIS of GFRP-RC, S-RC having jute fibers and GFRP-RC having jute fibers has increased to 118.56%, 254.64% and 305.15%, respectively. These results show that addition of jute fibers change the behavior of concrete against impact and the combination of GFRP-RC with jute fibers can sustain more impact as compared to others. The damage representation of remaining walls against both low and high impact are shown in Figure A.1 and Figure A.2, respectively.

Table 4.2: Comparison with previous study of JFRC.

Rebars	Ratio (JFRC to PC)	Previous Work Hussain and Ali [20]		Current Study	
		600 mm	900 mm	Low Impact	High Impact
(1)	(2)	(3)	(4)	(5)	(6)
Steel	Initial Strength	1.7	1.67	1.75	1.39
	Ultimate Strength	1.32	1.52	1.35	2.55
GFRP	Initial Strength	-	-	2.23	1.66
	Ultimate Strength	-	-	3.02	2.57

Hussain and Ali [20] investigated the resistance of JFRC against impact loading. Slab panels were subjected to 1.5 kg hammer dropped from 600 mm and 900 mm height and number of blows were determined till failure. For 600 mm height the ratio of initial crack strength of JFRC with steel rebars to PC with steel rebars came out to be 1.7 whereas ratio of ultimate failure strength came out to be 1.32. For 900 mm height the ratio of initial crack strength of JFRC with steel rebars to PC with steel rebars came out to be 1.67 whereas ratio of ultimate failure strength came out to be 1.52. However, in this study the ratio of initial crack strength came out to be 1.75 whereas ratio of ultimate failure strength came out to be 1.35 for prototypes reinforced with steel rebars against low impact. And against high impact the ratio of initial crack strength came out to be 1.39 whereas ratio of ultimate failure strength came out to be 2.55. As both the studies are based on relative comparison between PC and JFRC prototypes, the results seem to be agreeable. The comparison of results obtained is shown in Table 4.2.

The addition of Fibers in concrete results in better performance in terms of impact strength, impact energy absorption, penetration depth, crack patterns and loss of concrete volume [28–31]. Similarly, the increment in impact strength of FRC as compared to PC is in good agreement with the impact testing results of FRC conducted previously by researchers shown in Table 2.1.

4.2.2 Fundamental Period and Damping at Initial and Ultimate Damage Stages

Figure 4.3 shows the impact force time history of hammer and acceleration time history of back response of the wall at first impact strike, at impact strike leading to initial failure and at impact strike leading to ultimate failure. Development of cracks are also presented to relate the visual condition of steel rebars reinforced concrete wall tested against high impact. It can be seen that as the damage in wall has increased, fundamental frequency has decreased and damping percentage has increased. Damping ratios have been calculated by log decrement method. Table 4.3 shows the impact force generated by hammer, its response on back side of the walls and calculated fundamental periods with damping percentages. It can be seen that for low impact, acceleration recorded at the back of walls is greater for GFRP-RC walls having jute fibers, followed by GFRP-RC, S-RC having jute fibers and S-RC walls. Up to ultimate strength, the fundamental period has decreased more in case of S-RC walls having jute fibers that is 18.8 Hz than 23 Hz of S-RC walls and 20 Hz of GFRP-RC walls having jute fibers than 23.1 Hz of GFRP-RC walls. But, at ultimate strength the damping percentage of GFRP-RC walls having jute fibers is greater that is 9.3% than 8.9% of S-RC having jute fibers, followed by 8.1% of GFRP-RC and 5.6% of S-RC walls.

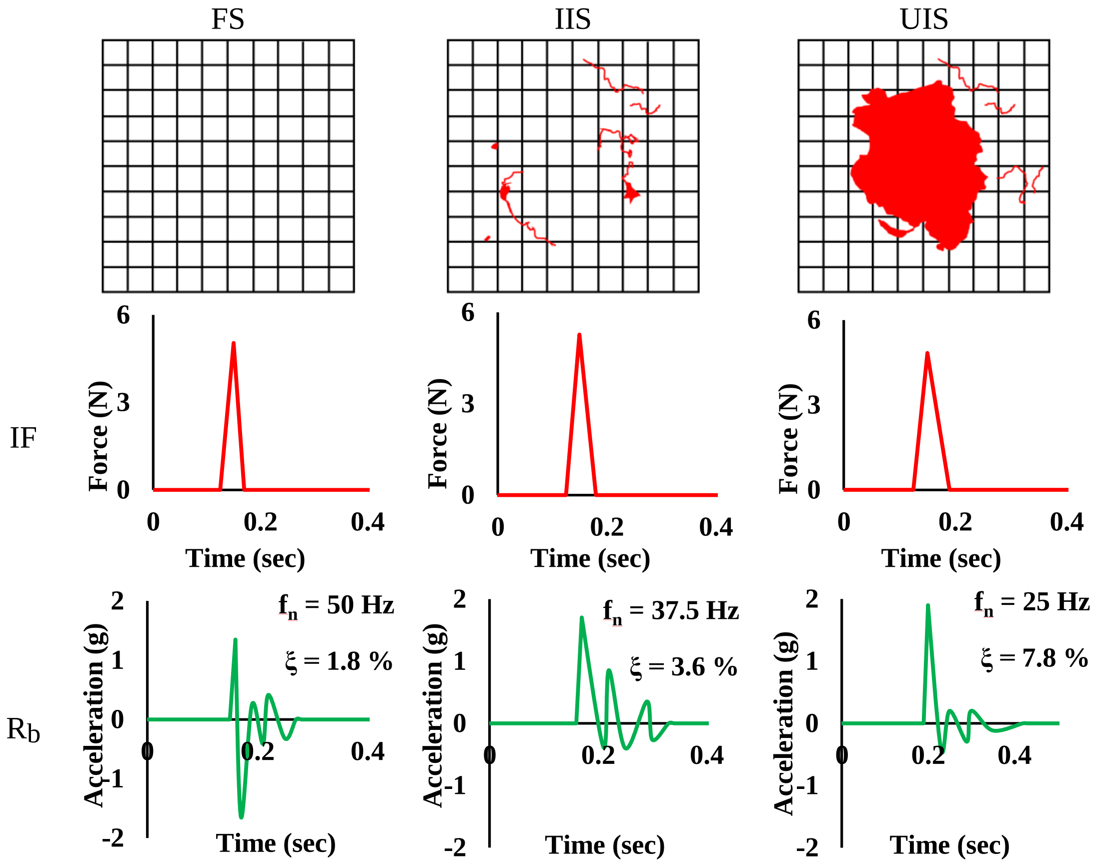

FIGURE 4.3: Applied force (Pi) and acceleration time response at back (R_b) side of S-RC wall with high impact for first strike (FS), at initial impact strength (IIS) and at ultimate impact strength (UIS).

For high impact, there is a significant decrease in the acceleration recorded at the back of walls than against low impact. It can be seen that acceleration is greater for GFRP-RC walls having jute fibers, followed by GFRP-RC, S-RC having jute fibers and S-RC walls. Up to ultimate strength, the fundamental period has decreased more in case of S-RC walls having jute fibers that is 15 Hz than 25 Hz of S-RC walls and 23.1 Hz of GFRP-RC walls having jute fibers than 30 Hz of GFRP-RC walls. However, at ultimate strength the damping percentage of GFRP-RC walls having jute fibers is greater that is 14.2% than 13.1% of S-RC having jute fibers, followed by 12.4% of GFRP-RC and 7.8% of S-RC walls. This shows the effectiveness of jute fibers in reducing the fundamental period of impact response and increasing the post impact residual strength. The low acceleration response against high impact shows the concentration of impact stress near the point of impact and gradual decrease of impact stress towards edges of walls.

TABLE 4.3: Effect of impact response on fundamental period and damping.

Test	Specimen	IF (N)	R_b (g)			f_n (Hz)			ξ (%)		
			FS	IIS	UIS	FS	IIS	UIS	FS	IIS	UIS
(1)	(2)	(3)	(4)	(5)	(6)	(7)	(8)	(9)	(10)	(11)	(12)
Low Impact	S-RC	5.02	0.78	0.52	0.27	35.5	33	23	1.8	3.3	5.6
	S-RC + JF	5.10	1.34	0.54	0.37	37.5	27.3	18.8	3.1	5.3	8.9
	GFRP-RC	5.10	2.34	1.40	0.68	30	27.7	23.1	2.7	4.8	8.1
	GFRP-RC + JF	4.98	2.71	1.54	0.78	50	25	20	5.8	6.9	9.3
High Impact	S-RC	6.74	1.55	0.89	0.61	50	37.5	25	1.8	3.6	7.8
	S-RC + JF	6.78	1.63	1.24	0.66	41.4	33	15	8.9	9.6	13.1
	GFRP-RC	6.64	2.17	1.15	0.89	42.9	37.5	30	2.3	7.4	12.4
	GFRP-RC + JF	6.85	2.58	1.72	0.94	42.9	33.3	23.1	6.7	8.7	14.2

4.3 Dynamic Properties at Different Damage Stages

Table 4.4 shows the consequences of low impact on walls before impact test, after initial impact strength failure and after ultimate impact strength failure. The damping ratios are determined to have a better understanding about the internal concrete damage due to impact. It can be observed that resonance frequencies before any impact test are greater in case of S-RC and GFRP-RC walls having jute fibers than S-RC and GFRP-RC walls and this trend continued till dynamic test conducted after ultimate failure. Similarly, the dynamic elastic modulus of S-RC and GFRP-RC walls before any impact test is greater than S-RC and GFRP-RC walls but after ultimate failure the dynamic elastic modulus of S-RC walls having jute fibers came out to be less than S-RC walls. However, GFRP-RC walls having jute fibers showed greater dynamic elastic modulus than GFRP-RC walls after ultimate failure. The trend shows that damping of every wall has increased as the impact strength is utilized.

Table 4.5 shows the consequences of high impact on walls before impact test, after initial impact strength failure and after ultimate impact strength failure. It can be observed that resonance frequencies before any impact test are greater in case of S-RC and GFRP-RC walls having jute fibers than S-RC and GFRP-RC walls and this trend continued till dynamic test conducted after ultimate failure except transverse frequency of S-RC walls that is greater than S-RC walls having jute fibers after ultimate failure. Similarly, the trend of dynamic elastic modulus is same as obtained for low impact except for S-RC walls that have more dynamic elastic modulus than S-RC walls having jute fibers after ultimate failure. Likewise, trend shows that damping of every wall has increased as the impact strength is utilized.

Table 4.4: Consequences of low impact on dynamic properties of walls.

Specimen	Stage	RF_l (Hz)	RF_t (Hz)	RF_r (Hz)	EM_d (GPa)	ξ (%)
(1)	(2)	(3)	(4)	(5)	(6)	(7)
S-RC	Before Impact	2485.5 ± 177.5	2485.5 ± 88.5	1464.5 ± 88.5	8.8 ± 1.2	1.7 ± 0.2
	After IIS	1464 ± 0	1775 ± 89	1043 ± 466	5.5 ± 0.6	2.4 ± 0.4
	After UIS	1242.5 ± 88.5	1486.5 ± 22.5	621.4 ± 44.4	3.9 ± 0.6	3.0 ± 0.6
S-RC + JF	Before Impact	2574 ± 533	3617 ± 555	2307.5 ± 44.5	17.5 ± 1.6	1.3 ± 0.3
	After IIS	2130.5 ± 976.5	2374 ± 111	1619.5 ± 377.5	7.6 ± 2.3	3.1 ± 0.1
	After UIS	1020.8 ± 44.3	1198.1 ± 843	865.6 ± 111	3.4 ± 0.2	4.3 ± 0.7
GFRP-RC	Before Impact	1242.5 ± 177.5	2108 ± 200	1264.5 ± 199.5	10.6 ± 0.4	1.4 ± 0.1
	After IIS	1064.5 ± 44.5	1286.5 ± 177.5	1064.5 ± 44.5	5 ± 1.3	3.7 ± 0.1
	After UIS	1042.5 ± 22.5	957.2 ± 113.9	1042.5 ± 22.5	3 ± 0.1	4.8 ± 0.5
GFRP-RC + JF	Before Impact	3572.5 ± 155.5	3772.5 ± 44.5	3107 ± 222	12.1 ± 0.4	3.1 ± 0.0
	After IIS	3129 ± 111	3573 ± 22	1975 ± 910	11.2 ± 0.2	4.0 ± 0.1
	After UIS	1731.1 ± 799	3328.5 ± 88.5	1708.9 ± 821.2	7.1 ± 2.4	6.1 ± 0.4

Table 4.5: Consequences of high impact on dynamic properties of walls.

Specimen	Stage	RF_l (Hz)	RF_t (Hz)	RF_r (Hz)	EM_d (GPa)	ξ (%)
(1)	(2)	(3)	(4)	(5)	(6)	(7)
S-RC	Before Impact	2196.5 ± 66.5	2596 ± 244	2196.5 ± 66.5	7.9 ± 0.8	2.2 ± 0.1
	After IIS	1619.5 ± 155.5	2063.5 ± 155.5	1198.5 ± 399.5	4.1 ± 0.3	3.4 ± 0.8
	After UIS	1042.9 ± 599.1	1730.5 ± 177.5	599.2 ± 111	2.8 ± 0.2	4.2 ± 0.6
S-RC + JF	Before Impact	2951 ± 333	3528.5 ± 155.5	3528.5 ± 155.5	18.7 ± 5.7	1.4 ± 0.1
	After IIS	1930.5 ± 821.5	2330 ± 377	1507.5 ± 87.5	8 ± 0.5	4.4 ± 2.3
	After UIS	1064.9 ± 399.1	1564.25 ± 55.25	1065.3 ± 133.2	2 ± 1.9	5.4 ± 2.1
GFRP-RC	Before Impact	2196.5 ± 643.5	2773.5 ± 66.5	2618.5 ± 221.5	5.8 ± 1.1	3.4 ± 1.9
	After IIS	1753 ± 244	1908.5 ± 266.5	2161 ± 75	2.2 ± 0.6	4.3 ± 1.3
	After UIS	909.5 ± 332.5	1486.5 ± 22.5	1442.5 ± 66.5	1.2 ± 0.2	6.0 ± 0.4
GFRP-RC	Before Impact	2729.5 ± 377.5	2884.5 ± 44.5	2996 ± 111	21 ± 0.7	4.3 ± 1.2
+ JF	After IIS	2663 ± 355	2774 ± 22	2263.5 ± 88.5	18.8 ± 0	6.9 ± 0.9
	After UIS	1819.5 ± 266.5	2218.5 ± 399.5	1731 ± 222	16.3 ± 0.7	7.1 ± 1.8

Figure 4.4a shows the percentage decrement in dynamic elastic modulus and the percentage increment in damping of walls against low impact, after IIS and after UIS. The value of EM_d and damping before impact test is taken as reference to be 100%. The EM_d of GFRP-RC having jute fibers decreased to 92.6% after IIS and to 58.7% after UIS. Similarly, EM_d of GFRP-RC decreased to 47.2% after IIS and to 28.3% after UIS. However, EM_d of S-RC having jute fibers decreased to 43.4% after IIS and to 19.4% after UIS. Similarly, EM_d of S-RC decreased to 62.5% after IIS and to 44.3% after UIS. The damping of S-RC and S-RC having jute fibers after UIS came out to be 3.0% and 4.3%, respectively. The damping of GFRP-RC and GFRP-RC having jute fibers after UIS came out to be 4.8% and 6.1%, respectively. In terms of increment in damping against low impact, GFRP-RC has performed better followed by S-RC having jute Fibers, GFRP-RC having jute fibers and S-RC.

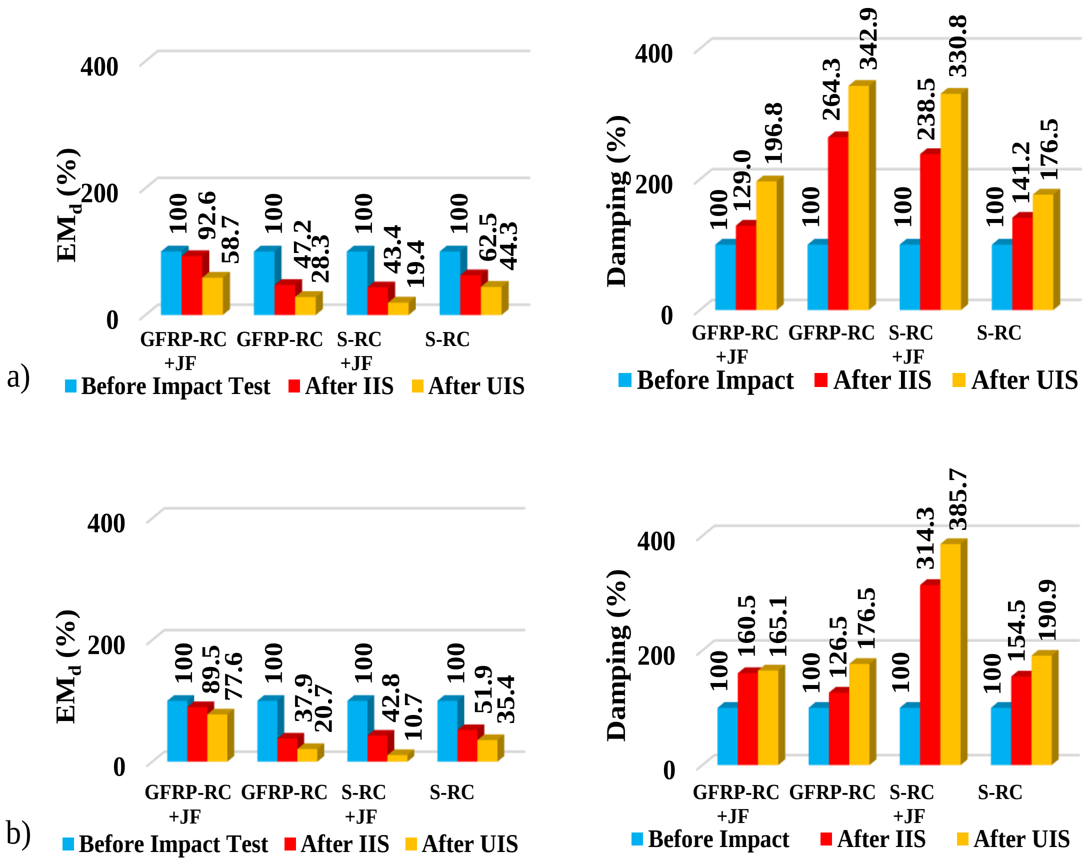

FIGURE 4.4: Percentage decrement in dynamic elastic modulus; a) against low impact, b) against high impact.

Figure 4.4b shows the percentage decrement in dynamic elastic modulus and the percentage increment in damping of walls against high impact, after IIS and after UIS. The value of EM_d and damping before impact test is taken as reference to be 100%. The value of EM_d before impact test is taken as 100%. The EM_d of GFRP-RC having jute fibers decreased to 89.5% after IIS and to 77.6% after UIS. Similarly, EM_d of GFRP-RC decreased to 37.9% after IIS and to 20.7% after UIS. However, EM_d of S-RC having jute fibers decreased to 42.8% after IIS and to 10.7% after UIS. Similarly, EMd of S-RC decreased to 51.9% after IIS and to 35.4% after UIS. The damping of S-RC walls and S-RC walls having jute fibers after UIS came out to be 4.2% and 5.4%, respectively. The damping of GFRP-RC walls and GFRP-RC walls having jute fibers after UIS came out to be 6.0% and 7.1%, respectively. In terms of increment in damping against high impact, S-RC having jute fibers has performed better followed by S-RC, GFRP-RC and GFRP-RC having jute fibers.

4.4 SEM Analysis for Damaged Surfaces on JFRC Wall Specimens

After impact testing, damaged walls are analyzed using SEM imaging. Figure 4.5a shows the post-impact fiber concrete debonding. The concrete matrix fractured around the fiber due to vibrational impact of hammer transferred throughout the wall. Concrete due to its brittle nature experienced cracking and lost the adhesion with fiber surface creating a peripheral cavity throughout the embedded length of fiber. Also, the impact strikes caused the separation of concrete surface and dispersal in fine particles. Figure 4.5b shows the condition of fiber from where the concrete separated due to the intensity of impact. A strong bond between fiber and concrete can be observed that led to the utilization of fiber strength against impact. Embedded fibers experienced shear failure during pull out that resulted in splitting of nano-strands. Fractured strand of fiber can be observed that resisted against the resultant of impact force acting perpendicular to its surface. The removal of concrete mass under the embedded fiber caused scratches on the fiber surface.

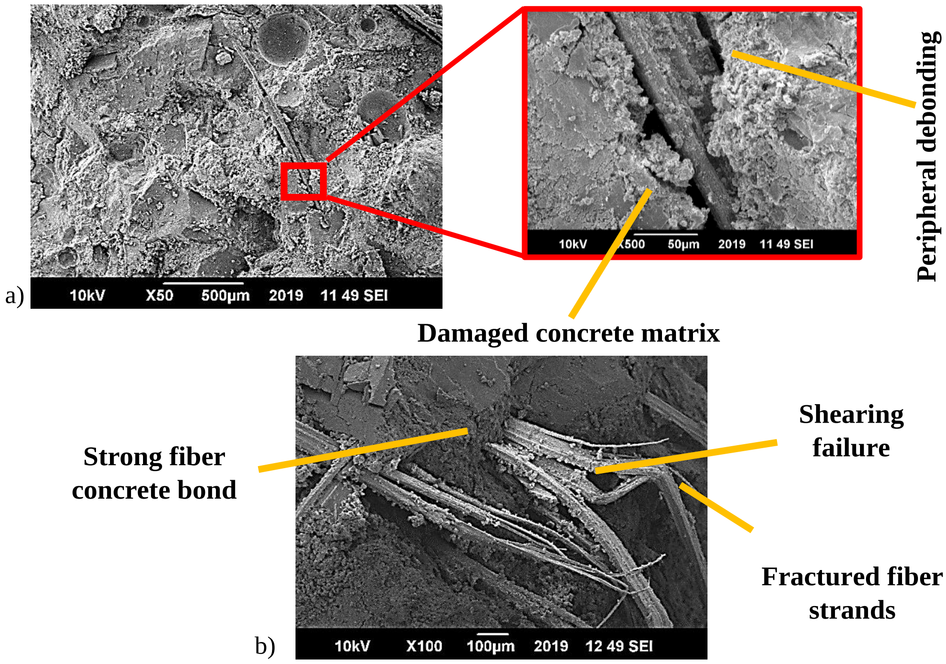

FIGURE 4.5: SEM analysis of failure zones under impact testing; a) post-impact Fiber concrete bond, b) fractured Fiber surface.

4.5 Summary

Walls are tested using modified pendulum approach. Two different masses are used to investigate impact resistance and basic dynamic properties. Accelerometers are used to record acceleration time history of impact. GFRP-RC walls having jute fibers have performed better as compared to GFRP-RC walls, S-RC walls having jute fibers and S-RC walls. SEM analysis shows fiber damage due to impact and strong bonding between concrete matrix and jute fibers.

Chapter 5

Discussion

5.1 Background

The experimental testing gave quantitative measurement of impact strength that has shown better performance of GFRP-RC reinforced concrete having jute fibres. The acceleration time graphs are utilized to investigate the response behavior of walls as the impact test proceeds. The behavior is then utilized for development of empirical relations to observe the trend of damping of material by its impact strength. Furthermore, moment and impact load capacity of walls have been investigated in this chapter.

5.2 Empirical Modeling for Relation between Damping and Strength at a Particular Impact

The damping of an element is directly related to its strength capacity of absorbing energy. Keeping in view the relation between them, experimental results of impact strength and obtained damping percentages are utilized to observe the trend by developing empirical relations.

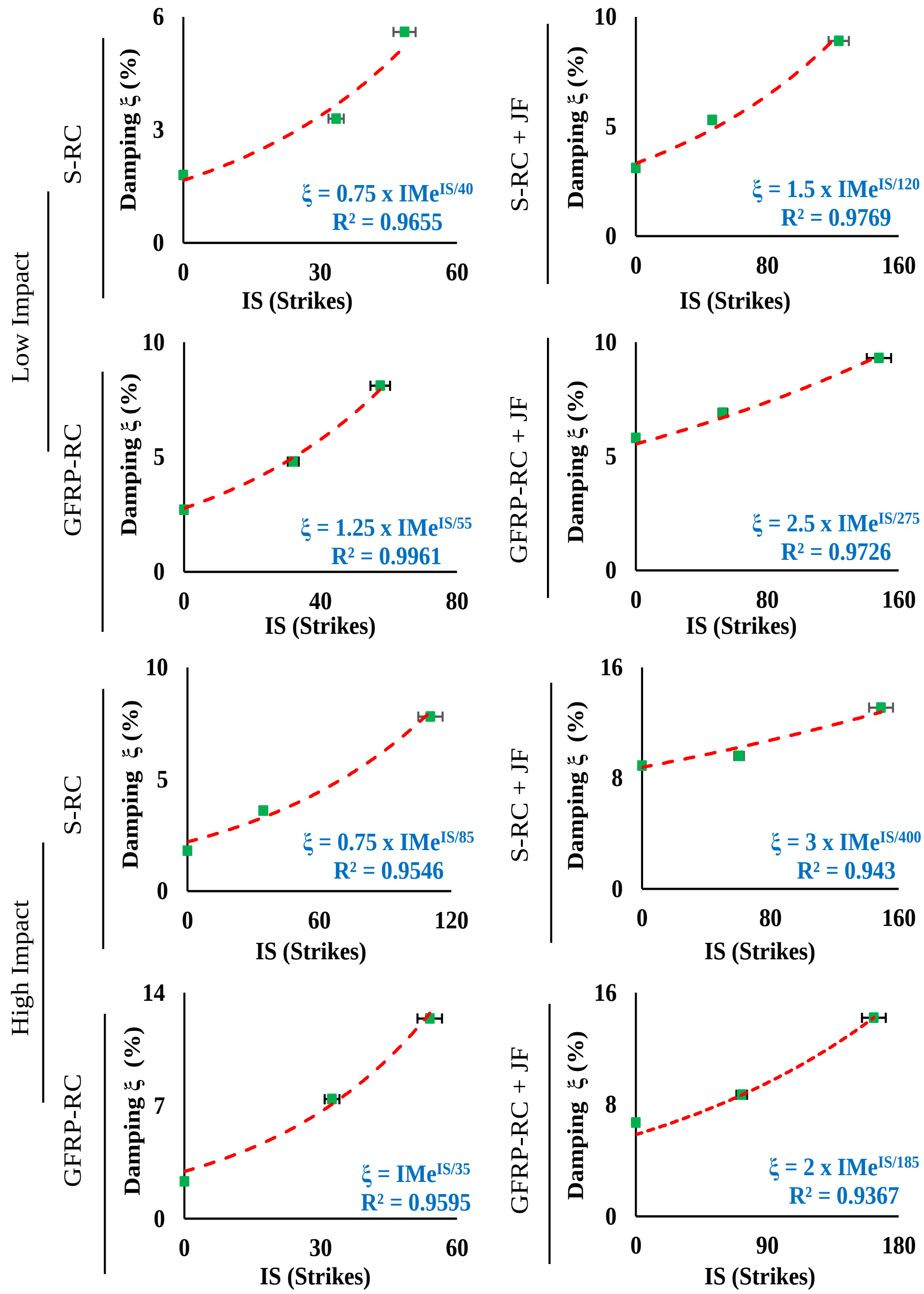

FIGURE 5.1: Development of empirical relation between impact strength (IS) and percentage damping against low and high impact.

For this purpose, graphs have been plotted separately for all combinations used in the test against low and high impact. Figure 5.1 shows the graphs of empirical relations developed between impact strength and percentage damping against low impact and high impact with obtained equations. The co-efficient of determination R^2 ranges from 93.6% to 99.6%. The generalized equation is as follows:

$$\xi = \alpha \times \mathrm{IMe}^{\mathrm{IS}/\beta} \tag{5.1}$$

Where IM is the impact mass and IS is impact strength (no. of strikes). Values of α are 0.75, 1.5, 1.25 and 2.5 for S-RC, S-RC + JF, GFRP-RC and GFRP-RC + JF, respectively against low impact. Similarly values of α are 0.75, 3, 1 and 2 for S-RC, S-RC + JF, GFRP-RC and GFRP-RC + JF, respectively against high impact. However, values of β are 40, 120, 55 and 275 for S-RC, S-RC + JF, GFRP-RC and GFRP-RC + JF, respectively against low impact. Similarly values of β are 85, 400, 35 and 185 for S-RC, S-RC + JF, GFRP-RC and GFRP-RC + JF, respectively against high impact.

Table 5.1: Comparison of experimental and empirical damping and percentage difference.

Test	Specimen	Experimental Damping		Empirical Damping		Percentage Difference	
		IIS	UIS	IIS	UIS	IIS	UIS
(1)	(2)	(3)	(4)	(5)	(6)	(7)	(8)
Low Impact	S-RC	3.3	5.6	3.8	5.6	15.1	0.3
	S-RC+JF	5.3	8.9	4.9	9.3	7.9	4.4
	GFRP-RC	4.8	8.1	5.0	7.9	3.2	2.8
	GFRP-RC+JF	6.9	9.3	6.7	9.5	2.7	2.0
High Impact	S-RC	3.6	7.8	3.3	8.0	8.9	3.1
	S-RC+JF	9.6	13.1	10.2	12.7	6.1	2.8
	GFRP-RC	7.4	12.4	7.4	13.7	0.0	9.8
	GFRP-RC+JF	8.7	14.2	8.7	14.1	0.5	0.6

Empirical equation is utilized to observe the damping trend of respective walls against their initial and ultimate strengths. Table 5.1 shows the results of damping obtained from experimental tests and empirical equations. Percentage difference is also reported to observe the accuracy of developed equation. The percentage difference between values of empirical damping and experimental damping against low impact ranges from 0.3% to 15.1%. Similarly, percentage difference between values of empirical damping and experimental damping against high impact ranges from 0% to 9.8%.

5.3 Analytical Modeling for Moment Capacity of Walls at Impact Location

The strength of concrete walls prepared using the combinations of reinforcement and jute fibers will have variation in resistance to impact load. So, in order to have an idea of their strengths, equations have been utilized to calculate their moment capacities. The moment capacity of walls, having combination of steel rebars with normal concrete, has been calculated using the formula given by [19]. However, the moment capacity of walls, having combination of steel rebars with JFRC, has been calculated using the formula given in equation 2.1. For moment capacity of walls having combination of GFRP rebars with normal concrete, equation 2.2 has been utilized. Likewise, the moment capacity of walls, having combination of GFRP rebars with JFRC, has been calculated using the formula given in equation 2.3. For impact load capacity, the formula given by [32] shown in Figure 2.1 cannot be directly applied on a 3-edge supported wall. So, the developed analytical equation for moment capacity at unit middle strip is utilized to calculate the impact load capacity at the center of 3-edge supported wall. In equation 5.2, 80% of the maximum moment reported by [32] is considered for 3-edge supported structure.

$$M_{I3S} = \left(1.1x^2 - \frac{x}{11}\right) \times 0.8\frac{PL}{12} \qquad \textit{for } 0 \le x \le h \tag{5.2}$$

where h is the vertical height proportion of the wall = height considered/total height and L is the horizontal span.

Table 5.2 shows the moment and impact load capacities of walls tested in this study.

Table 5.2: Comparison of moment and impact load capacities.

Specimen	f_y Steel rebar MPa	f_{fu} GFRP rebar MPa	PC MPa	f_c' JFRC MPa	T_f JF kN	M_{I3S} kN-m	P_i kN	Increment (%)
(1)	(2)	(3)	(4)	(5)	(6)	(7)	(8)	(9)
S-RC	537.52	-	14.66	-	-	4.64	795.7	-
S-RC+JF	537.52	-	-	11.33	5.13	4.69	803.6	1.1
GFRP-RC	-	756.94	14.66	-	-	5.24	898.0	12.9
GFRP-RC+JF	-	756.94	-	11.33	5.13	5.48	939.1	18.1

Note:

For S-RC + JF: $M_n = \left[\rho bdfy \times \left(d - \frac{\beta c}{2}\right)\right] + T_f\left(\frac{d+c-\beta c}{2}\right)$ Hussain and Ali [20]

For GFRP-RC: $M_n = A_f f_{fu} \times \left(d - \frac{\beta_1 c_b}{2}\right)$ ACI 440.1R-06 [26]

For GFRP-RC +JF: $M_n = A_f f_{fu} \times \left(d - \frac{\beta_1 c_b}{2}\right) + T_f\left(\frac{d+c-\beta c}{2}\right)$ Ejaz and Ali [27]

Tensile strength test was performed for the rebars used in this study, the f_y of steel rebars came out be 532.52 MPa and f_{fu} of GFRP rebars came out to be 756.94 MPa. The $f_{c'}$ of normal concrete came out to be 14.66 MPa and that of JFRC came out to be 11.33 MPa. The value of T_f is taken as 5.13 kN as 75% of flexural load taken by JFRC beamlet. The moment capacity of S-RC wall having jute fibers came out to be 4.69 kN-m while the moment capacity of S-RC wall came out to be 4.64 kN-m. However, the moment capacity of GFRP-RC wall came out to be 5.24 kN-m and moment capacity of GFRP-RC wall having jute fibers came out to be 5.48 kN-m. Similarly, the impact load capacity of S-RC wall having jute fibers came out to be 803.6 kN and that of S-RC wall came out to be 795.7 kN. Likewise, the impact load capacity of GFRP-RC wall came out to be 898.0 kN and that of GFRP-RC wall having jute fibers came out to be 939.1 kN. There is an increase of 1.1% in moment and impact load capacity of walls of S-RC wall due to addition of jute fibers. However, if GFRP rebars are used instead of steel rebars, the moment and impact load capacity of walls increase up to 12.9%. If steel rebars are replaced by GFRP rebars along with addition of jute fibers, the moment capacity of wall increases up to 18.1%. So, in terms of load carrying capacity, the combination of GFRP rebars with JFRC dominates, followed by GFRP rebars with normal concrete, steel rebars with JFRC and steel rebars with normal concrete.

5.4 Utilization of Research Outcome in Real Life Applications

The impact strength of GFRP rebars reinforced concrete having jute fibers has dominated over other combinations. Similarly, greater damping has been observed in GFRP-RC + JF walls at different failure stages. Post-impact fiber condition and bond between fiber concrete matrix shows better resistance against spalling. The greater moment capacity of GFRP-RC wall having jute fibers also justifies the role of fibers and GFRP rebars in possible flexural resistance against impact loading.

The greater impact strength of GFRP rebars reinforced concrete having jute fibers has established a safe ground for its practical utilization. As the security check posts and cabins are considered as temporary structures, the compromised strength of JFRC with enhanced toughness justifies its significance in constructing such single-story structures that most likely experience demolishing and relocation after a certain period of time as per the changing requirements. Therefore, the walls made up of GFRP rebars reinforced concrete having jute fibers are more likely to perform better keeping in mind the expensive blast walls for constructing the security check points meant for short term service duration.

5.5 Summary

The empirical equation developed shows good agreement of damping trend in relation to impact strength. The results from empirical equations and experimental testing are compared and percentage differences are calculated that came out to be in a reasonable range. Moment capacities and impact load capacities of walls are calculated for a 3-edge supported wall.

Chapter 6

Conclusion and Future Work

6.1 Conclusion

In current study, addition of agricultural waste jute fibers in concrete is focused in combination with steel rebars and GFRP rebars for application in concrete walls to investigate the strength in terms of resistance against impact loading. Mix design ratio of 1: 2: 3 (Cement: Sand: Aggregates) is used along with 0.6 w/c ratio. Jute fibers of 50 mm length are added, 5% by mass of cement. Rebars of diameter 6 mm are used. The outcomes of S-RC are taken as reference for comparison with outcomes for other combinations in terms of percentage increment and decrement. A reference value of 100% has been assigned to outcomes of S-RC. It is being obtained by dividing with its own value and multiplying by 100. However, values of other combinations have been divided by value of S-RC and multiplied by 100. The conclusions drawn from the conducted research are as follows:

- The greater toughness index of JFRC shows its dominance over PC in post-cracking energy absorption capacity.
- The combination of GFRP rebars reinforced concrete having jute fibers in walls can perform better in terms of resistance against low and high impact to resist initial cracking failure and ultimate failure followed by steel rebars

reinforced concrete having jute Fibers, GFRP rebars reinforced concrete and steel rebars reinforced concrete.

- The greater initial and post failure damping shows effectiveness of jute fibers when added in GFRP rebars reinforced concrete and steel rebars reinforced concrete in improving the structural response of wall to impact loading.
- Developed empirical equations can be used to observe the trend of probable damping of a wall in relation to its impact strength (Number of Strikes).
- The GFRP rebars reinforced concrete walls having jute fibers give greater moment and impact load carrying capacity as compared to the ones having steel rebars.
- The fractured condition of fibers depict strong bond strength between jute fibers and concrete matrix that poses resistance against spalling.

6.2 Future Work

Thus, jute fibers have a potential to be used in reinforcing concrete in order to apply sustainable practices in construction industry.

- Experimentally obtained strength properties of fiber reinforced concrete should be used in FE modeling to investigate the response of walls against impact loading.
- Comparison of cavities formation after casting and after testing along with durability of jute fiber reinforced concrete, co-relation of impact mass and prototype mass and bond between concrete and GFRP rebars need to be investigated for practical application in construction sector.

Bibliography

[1] F. Liu, W. Feng, Z. Xiong, G. Tu, and L. Li, "Static and impact behaviour of recycled aggregate concrete under daily temperature variations," *Journal of Cleaner Production*, vol. 191, no. 12, pp. 283–296, 2018.

[2] V. Aune, E. Fagerholt, M. Langseth, and T. Brvik, "A shock tube facility to generate blast loading on structures," *International Journal of Protective Structures*, vol. 7, no. 3, pp. 640–366, 2016.

[3] P. D. Smith, "Blast walls for structural protection against high explosive threats: A review," *International Journal of Protective Structures*, vol. 1, no. 1, pp. 67–84, 2010.

[4] E. El-Salakawy, R. Masmoudi, B. Benmokrane, F. Brire, and G. Desgagn, "Pendulum impacts into concrete bridge barriers reinforced with glass fibre reinforced polymer composite bars," *Canadian Journal of Civil Engineering*, vol. 31, no. 4, pp. 539–552, 2004.

[5] M. V. Seica, J. A. Packer, and D. Z. Yankelevsky, "Blast and impact loading effects on glass and steel elements and materials," *Thin-Walled Structures*, vol. 134, pp. 384–394, 2019.

[6] H. Sadraie, A. Khaloo, and H. Soltani, "Dynamic performance of concrete slabs reinforced with steel and GFRP bars under impact loading," *Engineering Structures*, vol. 191, pp. 62–81, 2019.

[7] L. Jin, R. Zhang, X. J. Dou, G., and X. Du, "Experimental and numerical study of reinforced concrete beams with steel fibers subjected to impact

loading," *International Journal of Damage Mechanics*, vol. 27, no. 7, pp. 1058–1083, 2018.

[8] N. Sultana, S. Z. Hossain, M. S. Alam, M. M. A. Hashish, and M. S. Islam, "An experimental investigation and modeling approach of response surface methodology coupled with crow search algorithm for optimizing the properties of jute fiber reinforced concrete," *Construction and Building Materials*, vol. 243, p. 118216, 2020.

[9] R. Merli, M. Preziosi, A. Acampora, M. C. Lucchetti, and E. Petrucci, "Recycled fibers in reinforced concrete: A systematic literature review," *Journal of Cleaner Production*, vol. 248, p. 119207, 2020.

[10] M. Zakaria, M. Ahmed, M. Hoque, and A. Shaid, "A comparative study of the mechanical properties of jute fiber and yarn reinforced concrete composites," *Journal of Natural Fibers*, pp. 1–12, 2018.

[11] J. S. Kim, H. J. Lee, and Y. Choi, "Mechanical properties of natural fiber-reinforced normal strength and high-fluidity concretes," *Computers and Concrete*, vol. 11, no. 6, pp. 531–539, 2013.

[12] X. G. Li, Y. Lv, B. G. Ma, Q. B. Chen, X. B. Yin, and S. W. Jian, "Utilization of municipal solid waste incineration bottom ash in blended cement," *Journal of Cleaner Production*, vol. 32, pp. 96–100, 2012.

[13] H. F. Campos, N. S. Klein, J. Marques Filho, and M. Bianchini, "Low-cement high-strength concrete with partial replacement of portland cement with stone powder and silica fume designed by particle packing optimization," *Journal of Cleaner Production*, p. 121228, 2020.

[14] A. Chandel, T. Shah, T. Shah, and D. Varde, "A comparative strength study of coir fibre reinforced concrete (CFRC) over plain cement concrete (PCC)," *Journal of Mechanical and Civil Engineering (IOSR-JMCE)*, vol. 13, no. 2, pp. 95–97, 2016.

[15] T. Zhang, Y. Yin, Y. Gong, and L. Wang, "Mechanical properties of jute fiber-reinforced high-strength concrete," *Structural Concrete*, pp. 1–10, 2019.

[16] G. Ramakrishna and T. Sundararajan, "Impact strength of a few natural fibre reinforced cement mortar slabs: a comparative study," *Cement & Concrete Composites*, vol. 27, no. 5, pp. 547–553, 2005.

[17] M. S. Islam and S. J. Ahmed, "Influence of jute fiber on concrete properties," *Construction and Building Materials*, vol. 189, pp. 768–776, 2018.

[18] M. Affan and M. Ali, "Compressive behavior of jute fiber reinforced concrete under freeze-thaw cycles," in *Proceedings of International Civil Engineering and Architecture Conference*, Trabzon, Turkey, April 17-20. 2019, pp. 2405–2411.

[19] 318, *Building code requirements for structural concrete and commentary*, American Concrete Institute Std., 2014.

[20] T. Hussain and M. Ali, "Improving the impact resistance and dynamic properties of jute fiber reinforced concrete for rebars design by considering tension zone of FRC." *Construction and Building Materials*, vol. 213, pp. 592–607, 2019.

[21] F. B. A. Beshara, I. G. Shaaban, and T. S. Mustafa, "Nominal flexural strength of high strength fiber reinforced concrete beams," *Arabian Journal for Science and Engineering*, vol. 37, no. 2, pp. 291–301, 2012.

[22] W. J. Chin, Y. H. Park, J. R. Cho, J. Y. Lee, and Y. S. Yoon, "Flexural behavior of a precast concrete deck connected with headed GFRP rebars and UHPC," *Materials*, vol. 13, no. 3, p. 604, 2020.

[23] E. A. Ahmed, C. Dulude, and B. Benmokrane, "Concrete bridge barriers reinforced with glass fibre-reinforced polymer: static tests and pendulum impacts," *Canadian Journal of Civil Engineering*, vol. 40, no. 11, pp. 1050–1059, 2013.

[24] K. M. Hossain, S. Alam, M. S. Anwar, and K. M. Julkarnine, "Bond strength of fiber-reinforced polymer bars in engineered cementitious composites," in *Proceedings of the Institution of Civil Engineers-Construction Materials*, vol. 173, no. 1, 2020, pp. 15–27.

[25] A. Goldston, M. Remennikov and M. N. Sheikh, "Experimental investigation of the behaviour of concrete beams reinforced with GFRP bars under static and impact loading," *Engineering Structures*, vol. 113, pp. 220–232, 2016.

[26] 440.1R-15, *Guide for the design and construction of structural concrete reinforced with FRP bars*, American Concrete Institute Std.

[27] A. Ejaz and M. Ali, "Development of empirical relation for moment capacity of a concrete prototype bridge deck slab reinforced with GFRP rebars and jute fibers," in *Proceedings of 2nd International Conference on Sustainable Development in Civil Engineering*, MUET, Jamshoro, Pakistan, December 05-07 2019, p. 218.

[28] P. P. Li, H. J. H. Brouwers, and Q. Yu, "Influence of key design parameters of ultra-high-performance fiber reinforced concrete on in-service bullet resistance," *International Journal of Impact Engineering*, vol. 136, p. 103434, 2020.

[29] J. Liu, C. Wu, Y. Su, J. Li, R. Shao, G. Chen, and Z. Liu, "Experimental and numerical studies of ultra-high-performance concrete targets against high-velocity projectile impacts," *Engineering Structures*, vol. 173, pp. 166–179, 2018.

[30] W. Wang and N. Chouw, "Flexural behaviour of FFRP wrapped CFRC beams under static and impact loadings," *International Journal of Impact Engineering*, vol. 111, pp. 46–54, 2018.

[31] M. Mastali, A. Dalvand, and A. R. Sattarifard, "The impact resistance and mechanical properties of reinforced self-compacting concrete with recycled glass fibre reinforced polymers," *Journal of Cleaner Production*, vol. 124, pp. 312–324, 2016.

[32] T. M. Pham and H. Hao, "Prediction of the impact force on reinforced concrete beams from a drop weight," *Advances in Structural Engineering*, vol. 19, no. 11, pp. 1710–1722, 2016.

[33] 544.2R-89, *Measurement of properties of fiber reinforced concrete*, American Concrete Institute Std.

[34] S. Ahmed and M. Ali, "Impact resistance investigation of fiber reinforced concrete having GFRP rebars in last two decades," in *Proceedings of 2nd International Conference on Sustainable Development in Civil Engineering*, MUET, Jamshoro, Pakistan, December 05-07 2019, p. 214.

[35] M. Zineddin and T. Krauthammer, "Dynamic response and behavior of reinforced concrete slabs under impact loading," *International Journal of Impact Engineering*, vol. 34, no. 9, pp. 1517–1534., 2007.

[36] Z. Wu, P. Zhang, L. Fan, and Q. Liu, "Debris characteristics and scattering pattern analysis of reinforced concrete slabs subjected to internal blast loadsa numerical study," *International Journal of Impact Engineering*, vol. 131, pp. 1–16, 2019.

[37] D. B. Dittenber and H. V. GangaRao, "Critical review of recent publications on use of natural composites in infrastructure," *Composites Part A: Applied Science and Manufacturing*, vol. 43, no. 8, pp. 1419–1429, 2012.

[38] M. Ali, A. Liu, H. Sou, and N. Chouw, "Mechanical and dynamic properties of coconut fibre reinforced concrete," *Construction and Building Materials*, vol. 30, pp. 814–825, 2012.

[39] K. H. Mo, U. J. Alengaram, M. Z. Jumaat, S. P. Yap, and S. C. Lee, "Green concrete partially comprised of farming waste residues: A review," *Journal of Cleaner Production*, vol. 117, pp. 122–138, 2016.

[40] J. Mo, L. Zeng, Y. Liu, L. Ma, C. Liu, S. Xiang, and G. Cheng, "Mechanical properties and damping capacity of polypropylene fiber reinforced concrete

modified by rubber powder," *Construction and Building Materials*, vol. 242, p. 118111, 2020.

[41] M. A. Vicente, J. Mnguez, and D. C. Gonzlez, "Computed tomography scanning of the internal microstructure, crack mechanisms, and structural behavior of fiber-reinforced concrete under static and cyclic bending tests," *International Journal of Fatigue*, vol. 121, pp. 9–19, 2019.

[42] T. F. Lam and J. M. Yatim, "Mechanical properties of kenaf fiber reinforced concrete with different fiber content and fiber length," *Journal of Asian Concrete Federation*, vol. 1, no. 1, pp. 11–21, 2015.

[43] C143/C143M, *Standard test method for slump of hydraulic-cement concrete*, ASTM International Std., 2015.

[44] C215-02, *Standard test method for fundamental transverse, longitudinal, and torsional resonant frequencies of concrete specimens*, ASTM International Std., 2014.

[45] C39/C39M, *Standard test method for compressive strength of cylindrical concrete specimens*, ASTM International Std., 2015.

[46] C496/C496M, *Standard test method for splitting tensile strength of cylindrical concrete specimens*, ASTM International Std., 2011.

[47] C78/C78M, *Standard test method for flexural strength of concrete (using simple beam with third-point loading)*, ASTM International Std., 2016.

[48] H. Yalciner, "Structural response to blast loading: the effects of corrosion on reinforced concrete structures," *Shock and Vibration*, 2014.

Annexure A

Impact testing results (of remaining specimens)

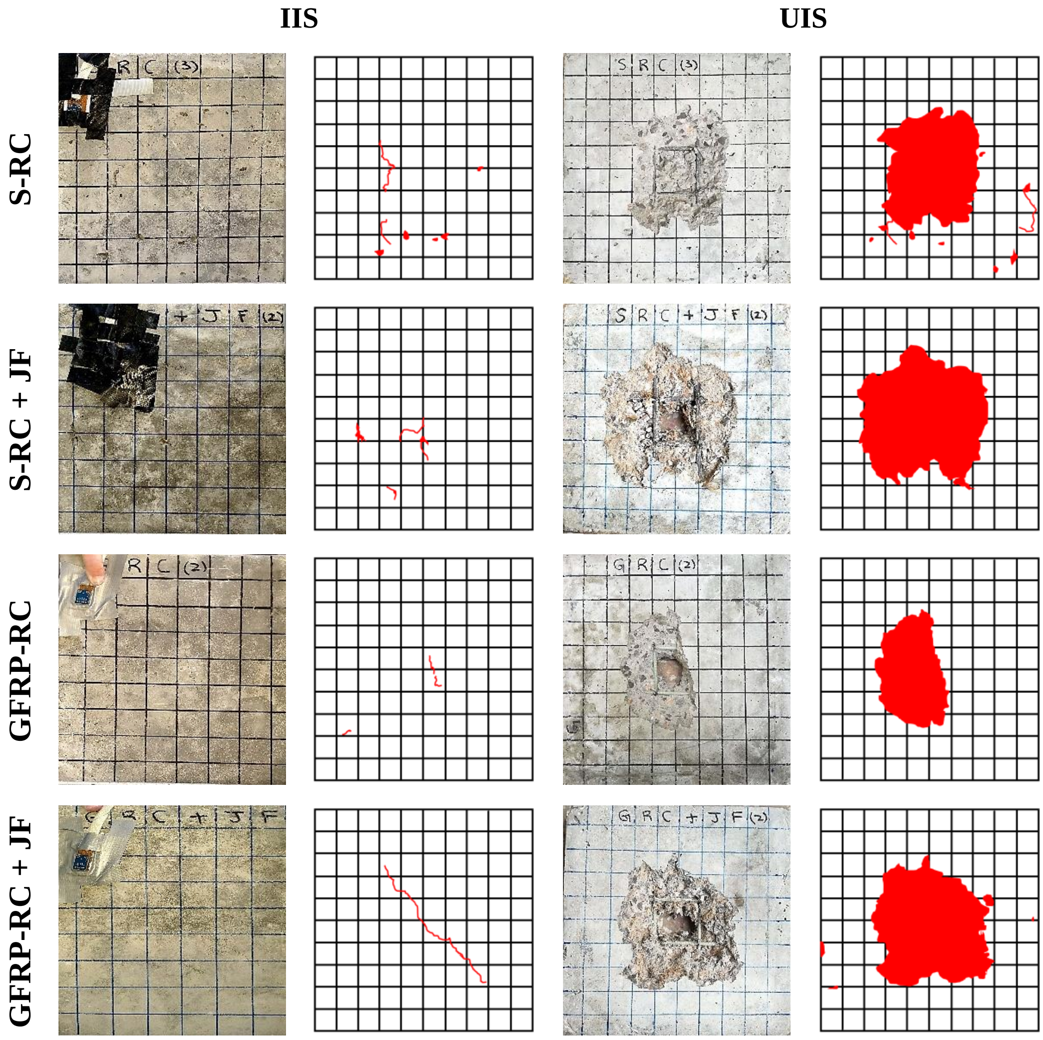

Figure A.1: Impact testing damage results of low impact.

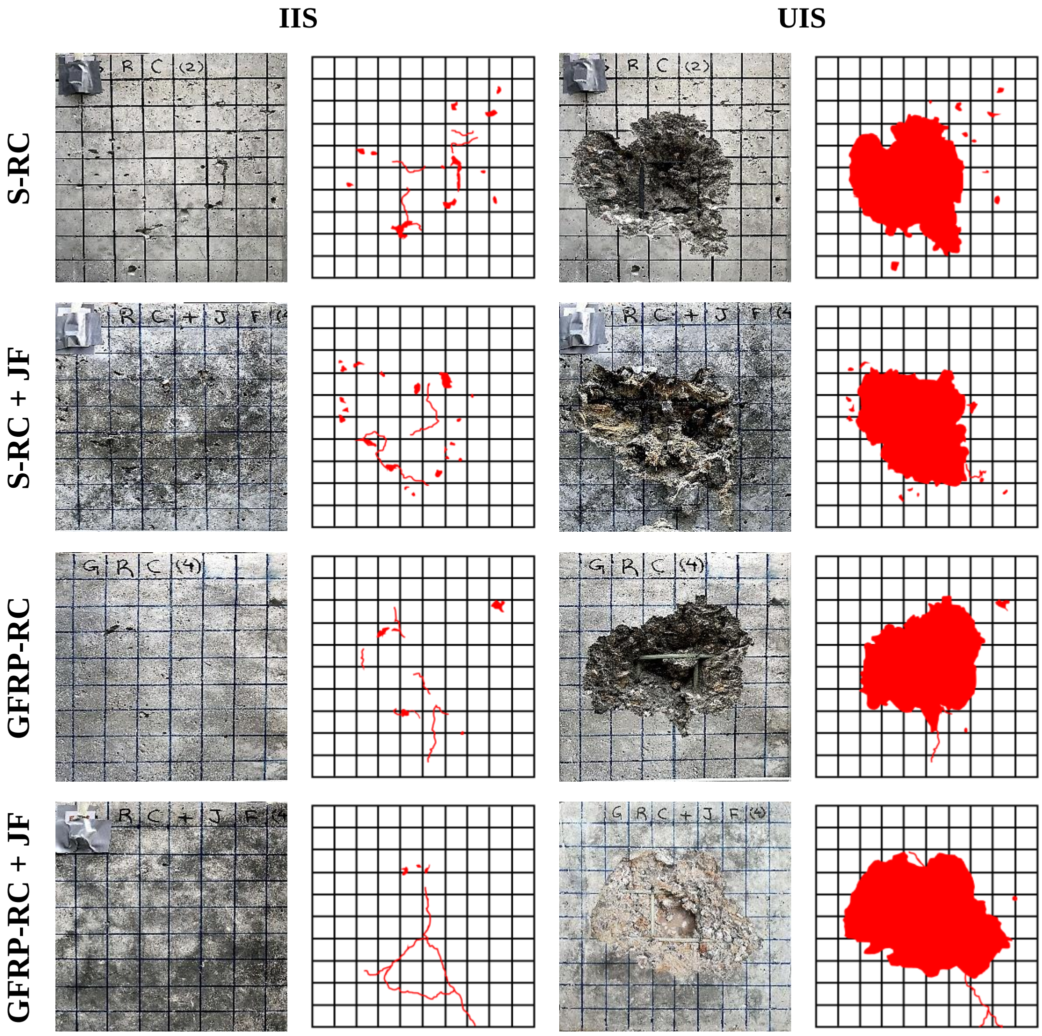

FIGURE A.2: Impact testing damage results of high impact.